Journal of Sound and Vibration (1997) **207**(1), 61–93

ACTIVE ISOLATION OF STRUCTURAL VIBRATION ON A MULTIPLE-DEGREE-OF-FREEDOM SYSTEM, PART I: THE DYNAMICS OF THE SYSTEM

P. Gardonio, S. J. Elliott and R. J. Pinnington

Institute of Sound and Vibration Research, University of Southampton, Southampton SO17 1BJ, England

(*Received* 8 *July* 1996, *and in final form* 19 *June* 1997)

This paper is the first of two companion papers concerning the active control of structural vibration in an isolator system. A preparatory study is reported of the passive vibration transmission, which is evaluated in terms of power, considering a multi-mount and multi-degree-of-freedom isolator system with passive mounts. The modelling of the system is based on a matrix method which uses mobility or impedance representations of three separate elements: the source of vibration, the receiver and the mounting system which connects the source to the receiver. A detailed description of the mobility or impedance formulae is given for a rigid mass oscillating in a plane (the source), for a beam on which flexural and longitudinal waves propagate (the mounts) and for an infinite or finite plate in which in-plane shear and longitudinal and out-of-plane flexural waves propagate (the receiver).

It is shown that at low frequencies any "rigid body mode" (axial-mode, transverse-mode, pitching-mode) is capable of transmitting considerable power to the receiving system, while the transmission of vibration at higher frequencies is mostly related to the dynamics of the distributed mounts or receiver.

1. INTRODUCTION

The active isolation of vibration generated by a source and transmitted to a receiver through active mounts has received much attention in recent years [1] and a great deal of progress has been achieved, particularly with actuator technology [2] and digital control systems [3]. These systems can sometimes achieve larger vibration reduction than traditional passive mounts, although the best isolation is generally obtained when an active system is used in combination with a passive mount. However, both the theoretical investigation and technology development of active isolation systems are still far from complete.

The theoretical aspects of the research are currently focused mainly in two areas: first, the study of the passive vibration transmission mechanism with no active control action; and, second, the investigation of the efficacy of different control strategies. The research carried out by the authors has been organized in exactly this way and, in this paper, a preparatory study regarding the mechanism of structural vibration transmission in an isolator is introduced, while in a companion paper [4] a systematic study concerning the effectiveness of different control strategies is presented. The contribution of this paper can be divided into two parts: first the formulation of the mathematical model of the isolator system; and, second, the use of the method to investigate the mechanism of structural vibration transmission. The mathematical model and the method of

0022–460X/97/410061 + 33 $25.00/0/sv971152

representing the vibration transmission adopted here allow some details of the vibration transmission to be described which have been found to be very significant for understanding the phenomenon that occurs when the isolator is provided with active mounts.

1.1. THE THEORETICAL MODEL

An active isolator system is generally composed of a source, free to vibrate in various ways, connected to a flexible receiver by several distributed active mounts. Examples of sources of vibration that could be isolated by using active mounts are car, ship and aeroplane engines or electric motors mounted into domestic machines (e.g., washing machines or refrigerators) or, finally, fans for air conditioning systems. These sources are usually mounted onto flexible cases or frames through soft suspensions which are capable of supporting the weight of the machine. A broad understanding of the dynamics of such complete isolator systems can be obtained by considering three frequency ranges [1]: the low, the intermediate and the high frequency ranges. The low frequency range is characterized by a few "rigid body" modes due to the source oscillations on the suspensions, while the intermediate frequency range is characterized by a higher number of modes, since the distributed mounts and the distributed receiver resonate. Usually, the source is a very stiff system that resonates only at higher frequencies. In these two frequency ranges the vibration of the system is usually described in terms of the global characteristics of the system by using a modal approach. Finally, in the high frequency range, the vibration of the receiver and mounts are dominated by the wave propagation phenomenon and the structural vibration of the system becomes more like the acoustic vibration which is usually described in terms of the scattering properties of the elements forming the system. von Flotow [5] has called the frequency limit at which the dynamics of the system move from a modal to a wave propagating behaviour the "acoustic limit".

It is not easy to find a model that is able to describe all of the phenomena occurring in the system over the whole of this frequency range. Single-degree-of-freedom models are not satisfactory and even models considering the presence of multiple mounts but modelling these as a lumped system are incomplete. Swanson *et al*. [6] have shown the limitations of modelling a complete isolator having several suspensions connecting a flexible distributed source and receiver with single-degree-of-freedom mounts. Sanderson *et al*. [7] and Petersson and Gibbs [8] have discussed the need to consider both the multi-mount and the multi-directional vibration transmission between a source and a receiver; in particular they emphasized the need to include both linear and rotational vibration transmission in the analysis.

In this paper a matrix model of the system has been developed, and particular attention has been devoted to the effects of multiple mounts and multi-degree-of-freedom vibration transmission. Point and transfer mobilities for the source and the receiver were used, while the dynamics of the mounts were specified by point and transfer impedances.

In particular, the case in which the source is a rigid mass which is free to move in a plane and is connected to an infinite or finite plate by a pair of active mounts has been studied in detail. Three wave types can propagate into the plate: in-plane longitudinal and shear waves and out-of-plane flexural waves. The mounts were modelled as a distributed one-dimensional system inclined at an arbitrary angle. Each mount was considered as a ring of rubber that reacts to axial and transverse displacements and to cross-sectional rotations. The control action was modelled as a pair of axial reactive forces acting at the top and bottom points of the mounts.

The matrix model presented in this paper can be used for a large variety of distributed mechanical, acoustical or coupled mechanical–acoustical systems characterized by a source transmitting vibration to a receiver through a number of paths. The "core" of the model is formed by the mobility or impedance matrices that are specific for each subsystem. In this paper the description of the matrix model has been developed by using a detailed formulation of the point and transfer mobility terms for a rigid mass (the source) and for a thin infinite or finite plate on which in-plane longitudinal and shear waves and out-of-plane flexural waves propagate (the receiver). Also reported is the formulation for the impedance terms of a beam in which flexural and longitudinal waves propagate (the mounts).

1.2. REPRESENTATION OF THE VIBRATION TRANSMISSION

When a multi-directional vibration transmission model is considered, a particular problem becomes apparent, since the structural vibration transmitted to the receiver is characterized by a large number of parameters that in some cases cannot be directly compared. Goyder and White [9–11] have used a novel approach to describe the vibration transmission in a complete isolator system. They represented the structural vibration transmitted to the receiver by using structural power, since this quantity can be used to quantify and compare all the components of the vibration. The first examples of quantifying structural vibration by using power were presented by Noiseux [12], Pavic [13], Verheij [14] and Williams *et al*. [15]. Other authors have also used this approach; for example, Pinnington and White [16] and Pinnington [17] have investigated the power transmission to a flexible receiver assuming simplified one-degree-of-freedom models of the mounts. Petersson [18, 19] and Koh and White [20–22] have emphasized the importance of both force and moment excitations in the power transmission to beam or plate-like structures. Rook and Singh [23] and Fastard and Singh [24] have studied power transmission in systems having several lumped members with multiple joints.

In this paper, the vibration transmitted to the flexible receiver through a number of distributed mounts is quantified by using structural power. The ability to compare the importance of different mechanisms in the vibration transmission to the receiver by using a power approach and the use of coupled multi-degree-of-freedom model give the possibility of producing a novel and detailed account of the dynamics of an isolator which simplified models cannot produce.

Power has also been used as a parameter to quantify the structural vibration transmission for two other reasons. First, in many cases the purpose of vibration isolation is to control the noise radiated by the receiver [25, 26]. The characterization of vibration transmission using power represents a good way to estimate the noise emitted by the receiver of a complete isolating system, since this quantity represents the energy available for causing radiated sound [27]. Second, one proposed strategy for active vibration control is the minimization of power transmission to the receiver [28]. This is an alternative to the conventional strategy of cancelling the velocities or forces at the junctions between the mounts and the receiver or minimizing the vibrational response of the receiver measured at several points. An investigation of the power transmission in a passive isolator system is thus required to understand the behaviour of a system in which power transmission is actively minimized.

The accuracy of the matrix model used here, and the method adopted to describe the vibrations, have allowed a detailed study of the vibration transmission in a complete isolating system. First of all, the analysis carried out shows the importance of considering a multi-mount and multi-degree-of-freedom model at low frequencies, since it has been

demonstrated that any "rigid body mode" resonance (axial mode, transverse mode or, pitching mode) is capable of transmitting a large quantity of vibration. Moreover, having modelled the mounts and the receiver as distributed systems has shown the trend of the vibration transmission in the mid-frequency range. In particular, the results show that for a finite plate, the first modes of the receiver greatly influence the transmission of vibration, which can be greater than in the case of a source rigidly fixed to the receiver. Finally, by using power it has been possible to evaluate and compare the contribution from each degree of freedom to the vibration transmission. The simulations have shown that at low frequency the power is mainly transmitted through axial vibration, but as the frequency rises the transmission of power tends to be equally distributed between axial and angular vibration.

2. GENERAL MODEL FOR MULTIPLE ACTIVE SUSPENSIONS

Many of the studies for complete isolators are concerned with systems having a single mount vibrating only in one direction [29, 30]. A more detailed study of the system is needed for a system with many mounts (usually three or four) and composed of distributed flexible members [31–33]. The finite element method can be used to study this problem, but the isolation model can be complicated and physical insight limited. Good results have been obtained by using an approach in which the system is divided into individual components (for a complete isolating system we consider three components: the source, the mounting system and the receiver) and each component is studied in terms of point and transfer mobilities or impedances [34, 35]. In reference [34] a matrix model is introduced in which the dynamics of the source and the receiver are expressed in terms of point mobility matrices and the dynamics of the mounting system connecting these two members is given in terms of the transfer mobility matrix. This formulation is valid for linear systems and can describe the dissipative effects of all three members, but was limited to axial motion only. In the following section this approach will be generalized for multi-axis vibration [36].

The complete isolating system is divided into three flexible parts as shown in Figure 1: the source, the mounting system, composed of n suspensions, and the receiver. These parts are connected at a finite number of junctions. At each junction, the motion and the forces transmitted are characterized by six parameters. These velocity and force parameters are grouped into a velocity junction vector and a force junction vector, which for the jth junction and at a single frequency can be written as

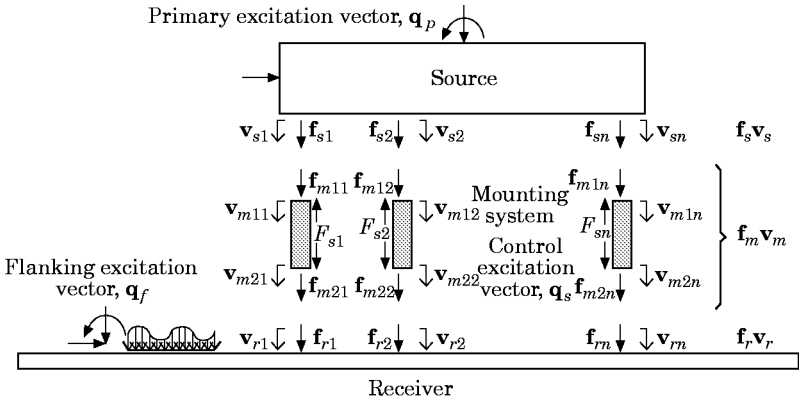

Figure 1. The scheme of a general complete isolating system.

$$\mathbf{v}_j \equiv \begin{Bmatrix} \dot{u}_j \\ \dot{v}_j \\ \dot{w}_j \\ \dot{\theta}_{xj} \\ \dot{\theta}_{yj} \\ \dot{\theta}_{zj} \end{Bmatrix}, \qquad \mathbf{f}_j \equiv \begin{Bmatrix} N_{xj} \\ N_{yj} \\ N_{zj} \\ M_{xj} \\ M_{yj} \\ M_{zj} \end{Bmatrix}, \tag{1, 2}$$

where $\dot{u}_j$, $\dot{v}_j$ and $\dot{w}_j$ are the complex linear velocities, respectively, along the x, y and z directions, $\dot{\theta}_{xj}$, $\dot{\theta}_{yj}$ and $\dot{\theta}_{zj}$ are the angular complex velocities referred, respectively, to the x-, y- and z-axes, and N_{xj}, N_{yj} and N_{zj} are the complex forces in the x, y and z directions and, finally, M_{xj}, M_{yj} and M_{zj} are the complex moments referred, respectively, to the θ_{xj}, θ_{yj} and θ_{zj} rotations. With reference to the notation shown in Figure 1, combinations of these junction vectors are then grouped together to form three combined pairs of vectors: the *source velocity vector* ($\mathbf{v}_s$) and *force vector* ($\mathbf{f}_s$), the *receiver velocity vector* ($\mathbf{v}_r$) and *force vector* ($\mathbf{f}_r$) and the *mounting system velocity vector* ($\mathbf{v}_m$) and *force vector* ($\mathbf{f}_m$). The source and receiver velocity vector and force vector are given by:

$$\mathbf{v}_s \equiv \begin{Bmatrix} \mathbf{v}_{s1} \\ \mathbf{v}_{s2} \\ \vdots \\ \mathbf{v}_{sn} \end{Bmatrix}, \qquad \mathbf{f}_s \equiv \begin{Bmatrix} \mathbf{f}_{s1} \\ \mathbf{f}_{s2} \\ \vdots \\ \mathbf{f}_{sn} \end{Bmatrix}, \tag{3, 4}$$

$$\mathbf{v}_r \equiv \begin{Bmatrix} \mathbf{v}_{r1} \\ \mathbf{v}_{r2} \\ \vdots \\ \mathbf{v}_{rn} \end{Bmatrix}, \qquad \mathbf{f}_r \equiv \begin{Bmatrix} \mathbf{f}_{r1} \\ \mathbf{f}_{r2} \\ \vdots \\ \mathbf{f}_{rn} \end{Bmatrix}, \tag{5, 6}$$

where $\mathbf{v}_{sj}$ and $\mathbf{f}_{sj}$ represent the velocity junction vector and the force junction vector at the source junction for the jth mount, while $\mathbf{v}_{rj}$ and $\mathbf{f}_{rj}$ represent the velocity junction vector and the force junction vector at the receiver junction for the jth mount. The mounting system velocity vector and force vector are given by

$$\mathbf{v}_m \equiv \begin{Bmatrix} \mathbf{v}_{m11} \\ \mathbf{v}_{m12} \\ \vdots \\ \mathbf{v}_{m1n} \\ \mathbf{v}_{m21} \\ \mathbf{v}_{m22} \\ \vdots \\ \mathbf{v}_{m2n} \end{Bmatrix}, \qquad \mathbf{f}_m \equiv \begin{Bmatrix} \mathbf{f}_{m11} \\ \mathbf{f}_{m12} \\ \vdots \\ \mathbf{f}_{m1n} \\ \mathbf{f}_{m21} \\ \mathbf{f}_{m22} \\ \vdots \\ \mathbf{f}_{m2n} \end{Bmatrix}, \tag{7, 8}$$

where $\mathbf{v}_{m1j}$ and $\mathbf{f}_{m1j}$ represent the velocity junction vector and the force junction vector at the source junction for the jth mount and $\mathbf{v}_{m2j}$ and $\mathbf{f}_{m2j}$ represent the velocity junction vector and the force junction vector at the receiver junction for the jth mount.

The dynamics of the source and the receiver are studied by using a mobility matrix approach, so that their velocity and force vectors can be written in the forms

$$\mathbf{v}_s = \mathbf{M}_{s1}\mathbf{f}_s + \mathbf{M}_{s2}\mathbf{q}_p, \qquad \mathbf{v}_r = \mathbf{M}_{r1}\mathbf{f}_r + \mathbf{M}_{r2}\mathbf{q}_f, \tag{9, 10}$$

where $\mathbf{M}_{s1}$, $\mathbf{M}_{s2}$ and $\mathbf{M}_{r1}$, $\mathbf{M}_{r2}$ are the mobility matrices, respectively, of the source and the receiver (see Appendices A and C), and $\mathbf{q}_p$, $\mathbf{q}_f$ are, respectively, the primary and flanking excitation vectors. The forces exciting the receiver could be due to a subsystem connected with it or to a flanking path connecting the source with the receiver. The dynamics of the mounting system are expressed using an impedance matrix approach,

$$\mathbf{f}_m = \mathbf{Z}_{m1}\mathbf{v}_m + \mathbf{Z}_{m2}\mathbf{q}_s, \tag{11}$$

where $\mathbf{Z}_{m1}$ and $\mathbf{Z}_{m2}$ are the impedance matrices of the mounting system (see Appendix B) and $\mathbf{q}_s$ is the control excitation vector. The source and receiver equations, (9) and (10), can be grouped together in one equation,

$$\mathbf{v}_{sr} = \mathbf{M}_{sr1}\mathbf{f}_{sr} + \mathbf{M}_{sr2}\mathbf{q}_{pf}, \tag{12}$$

where the two mobility matrices and the excitation vector have the forms:

$$\mathbf{M}_{sr1} = \begin{bmatrix} \mathbf{M}_{s1} & \mathbf{0} \\ \mathbf{0} & \mathbf{M}_{r1} \end{bmatrix}, \qquad \mathbf{M}_{sr2} = \begin{bmatrix} \mathbf{M}_{s2} & \mathbf{0} \\ \mathbf{0} & \mathbf{M}_{r2} \end{bmatrix}, \qquad \mathbf{q}_{pf} = \begin{Bmatrix} \mathbf{q}_p \\ \mathbf{q}_f \end{Bmatrix}, \tag{13–15}$$

and the junction *velocity* and *force vectors* are given by:

$$\mathbf{v}_{sr} \equiv \begin{Bmatrix} \mathbf{v}_s \\ \mathbf{v}_r \end{Bmatrix}, \qquad \mathbf{f}_{sr} \equiv \begin{Bmatrix} \mathbf{f}_s \\ \mathbf{f}_r \end{Bmatrix}, \tag{16, 17}$$

where $\mathbf{v}_{sr}$ and $\mathbf{f}_{sr}$ are called, respectively, the *source-receiver velocity vector* and *source-receiver force vector*. The source receiver vectors are related to the analogous mounting system vectors by a *transformation matrix* $\mathbf{T}$ in such a way as to satisfy the continuity principle (for the velocity vectors) and the equilibrium principle (for the force vectors) at each junction:

$$\mathbf{f}_m = -\mathbf{T}\mathbf{f}_{sr}, \qquad \mathbf{v}_m = \mathbf{T}\mathbf{v}_{sr}. \tag{18, 19}$$

These matrices are equal to unity for vertically arranged mounts but assume a more complicated form for inclined mounts (see Appendix D). By using these two relations, equations (11) and (12) can be related in such a way as to find the source–receiver velocity vector or the source-receiver force vector as a function of the primary and control sources:

$$\mathbf{v}_{sr} = \mathbf{Q}_{pv}\mathbf{q}_{pf} + \mathbf{Q}_{sv}\mathbf{q}_s, \qquad \mathbf{f}_{sr} = \mathbf{Q}_{pf}\mathbf{q}_{pf} + \mathbf{Q}_{sf}\mathbf{q}_s, \tag{20, 21}$$

where

$$\mathbf{Q}_{pv} = (\mathbf{I} + \mathbf{M}_{sr1}\mathbf{T}^{-1}\mathbf{Z}_{m1}\mathbf{T})^{-1}\mathbf{M}_{sr2}, \qquad \mathbf{Q}_{sv} = -(\mathbf{I} + \mathbf{M}_{sr1}\mathbf{T}^{-1}\mathbf{Z}_{m1}\mathbf{T})^{-1}\mathbf{M}_{sr1}\mathbf{T}^{-1}\mathbf{Z}_{m2}, \tag{22, 23}$$

$$\mathbf{Q}_{pf} = -\mathbf{T}^{-1}\mathbf{Z}_{m1}\mathbf{T}(\mathbf{I} + \mathbf{M}_{sr1}\mathbf{T}^{-1}\mathbf{Z}_{m1}\mathbf{T})^{-1}\mathbf{M}_{sr2}, \tag{24}$$

$$\mathbf{Q}_{sf} = \mathbf{T}^{-1}\mathbf{Z}_{m1}\mathbf{T}(\mathbf{I} + \mathbf{M}_{sr1}\mathbf{T}^{-1}\mathbf{Z}_{m1}\mathbf{T})^{-1}\mathbf{M}_{sr1}\mathbf{T}^{-1}\mathbf{Z}_{m2} - \mathbf{T}^{-1}\mathbf{Z}_{m2}. \tag{25}$$

The vibration transmission to the receiver will be quantified by using power and for the specific model investigated five types of power parameters can be defined: the *power input by the primary excitation on the source structure* $\mathbf{q}_p$, $\{P_p\}$; the *power input by the flanking*

excitation on the receiver structure $\mathbf{q}_f$, $\{P_f\}$; the *power input by the control excitation* $\mathbf{q}_s$, $\{P_s\}$, the *power transmitted to the receiver through the mounting system due to both the primary and control excitations*, $\{P_t\}$; and the *total power input into the receiver*, $\{P_r\}$.

The power input by the primary force on the source structure into the complete isolating system is given by:

$$P_p = \tfrac{1}{2}\mathrm{Re}\,(\mathbf{q}_p^{\mathrm{H}}\mathbf{v}_{sp}), \tag{26}$$

where $\mathbf{v}_{sp}$ is a vector containing the velocity parameters at the source points at which the primary excitations act, and it can be expressed as

$$\mathbf{v}_{sp} = \mathbf{M}_{sp1}\mathbf{q}_p + \mathbf{M}_{sp2}\mathbf{f}_s, \tag{27}$$

where $\mathbf{M}_{sp1}$ and $\mathbf{M}_{sp2}$ represent mobility matrices evaluated in a similar way as described in Appendix A. The power input into the complete isolating system by the flanking excitation is given by

$$P_f = \tfrac{1}{2}\mathrm{Re}\,(\mathbf{q}_f^{\mathrm{H}}\mathbf{v}_{rf}), \tag{28}$$

where $\mathbf{v}_{rf}$ is a vector containing the velocity parameters at the receiver points at which the flanking excitations act, and it can be expressed as

$$\mathbf{v}_{rf} = \mathbf{M}_{rf1}\mathbf{q}_f + \mathbf{M}_{rf2}\mathbf{f}_r, \tag{29}$$

where $\mathbf{M}_{rf1}$ and $\mathbf{M}_{rf2}$ are mobility matrices evaluated in a similar way as described in Appendix C. The power input into the complete isolating system due to the control source is given by

$$P_s = \tfrac{1}{2}\mathrm{Re}\,(\mathbf{q}_s^{\mathrm{H}}\bar{\mathbf{v}}_m), \tag{30}$$

where $\bar{\mathbf{v}}_m$ is a vector containing only the axial velocity at the junctions of the mounts. The power transmitted to the receiver by the primary and control excitations is given by

$$P_t = \tfrac{1}{2}\mathrm{Re}\,(\mathbf{f}_r^{\mathrm{H}}\mathbf{v}_r). \tag{31}$$

In the following sections the analysis of the power transmitted to the receiver will consider three components: the power associated with axial or out-of-plane displacements, the power associated with transverse or in-plane displacements and the power associated with rotations. The following convention will be used to define these power quantities. The power associated with axial displacement of the source junctions (w_s) or out-of-plane displacement of the receiver junctions (w_r) will be called the "axial component of power"; the power associated with transverse displacement of the source junctions (v_s) or in-plane displacement of the receiver junctions (v_r) will be called the "transverse component of power" and finally the power associated with rotation of the source junctions (θ_s) or receiver junctions (θ_r) will be called the "angular component of power". Finally, the total power input to the receiver is obtained by summing the power transmitted to the receiver by the source and the power input to the receiver by the flanking excitation

$$P_r = P_t + P_f = \tfrac{1}{2}\mathrm{Re}\,(\mathbf{f}_r^{\mathrm{H}}\mathbf{v}_r + \mathbf{q}_f^{\mathrm{H}}\mathbf{v}_{rf}). \tag{32}$$

The power transmitted to the receiver by the primary and the control excitations (P_t) or the power input into the receiver by the flanking excitation (P_f) could assume negative values, indicating an energy flow through the receiver directed to the source if P_t is negative or directed to the flanking source, that behaves as an absorber, if P_f is negative.

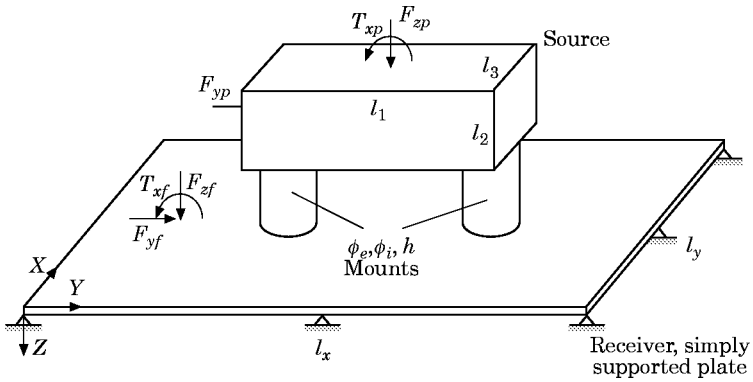

Figure 2. The complete isolating system.

3. MULTI-DEGREE-OF-FREEDOM COMPLETE ISOLATING SYSTEM WITH TWO ACTIVE MOUNTS

In this paper, we consider the vibration isolation of a source connected to a simply supported finite plate or to an infinite plate by a pair of active mounts. The active mounts have an arbitrary inclination β and can generate only axial control forces. This paper explores the passive dynamics of the system without considering the effects of the active control. In Figure 2 is shown the geometry of the system, while the dimensions and physical characteristics of the three members are summarized in Table 1.

The source is a rigid mass that is free to vibrate in the y–z plane. Its oscillations induce longitudinal and flexural waves into the distributed mounts which then cause in-plane longitudinal and shear waves and out-of-plane flexural waves in the distributed receiver plate.

TABLE 1

Main characteristics of the system

Model component	Parameter	Value
Source (aluminium)	Dimensions	$l_1 \times l_2 \times l_3 = 0{\cdot}52 \times 0{\cdot}3 \times 0{\cdot}25$ m
	Density	$\rho = 2700$ kg/m^3
	Mass	$m = 105{\cdot}3$ kg
	Moment of inertia	$I_G = 3{\cdot}16$ kg m^2
Passive mounts (soft rubber)	External diameter	$\phi_e = 6$ cm
	Internal diameter	$\phi_i = 3$ cm
	Height	$h = 10$ cm
	Moment of inertia	$I_x = 5{\cdot}96 \times 10^{-7}$ m^4
	Density	$\rho = 1000$ kg/m^3
	Young's modulus of elasticity	$E = 1 \times 10^7$ N/m^2
	Poisson ratio	$\nu = 0{\cdot}33$
	Loss factor	$\eta = 0{\cdot}1$
Receiver (aluminium)	Finite plate dimensions	$l_x \times l_y = 1 \times 1{\cdot}5$ m
	Thickness	$s = 0{\cdot}5$ cm
	Density	$\rho = 2700$ kg/m^3
	Young's modulus of elasticity	$E = 7{\cdot}1 \times 10^{10}$ N/m^2
	Shear modulus of elasticity	$G = 2{\cdot}4 \times 10^{10}$ N/m^2
	Poisson ratio	$\nu = 0{\cdot}33$
	Loss factor	$\eta = 0{\cdot}02$

The block mass is assumed to be excited by an axial (F_{zp}) and a transverse (F_{yp}) force and by a torque (T_{xp}). These three components are sufficient to reproduce a general source of vibration acting on the block mass. The receiver plate is excited by the two sets of forces–moments at the junctions (N_{yr1}, N_{zr1}, M_{xr1} and N_{yr2}, N_{zr2}, M_{xr2}) and by the flanking excitation (F_{yf}, F_{zf}, M_{xf}). The junctions connecting the two mounts to the receiver and the flanking excitation are all assumed to be along a line parallel to the y-axis at $x = l_x/2$. The receiver plate is assumed to be either infinite, or finite with simply supported boundary conditions. The mounts are assumed to be cylinders with internal control forces (F_{s1}, F_{s2}) acting at either end. The details of the actuators that generate these forces are not modelled. All excitations acting on the complete isolator system are considered harmonic with time dependence $\exp(j\omega t)$.

The study of the passive isolation of this system can give some preliminary indications of the main problems for the simultaneous control of different types of vibration induced by a source into a flexible receiver.

3.1. THE MATRIX MODEL

The individual expressions required as the elements in the matrix model are derived in Appendixes A, B, C and D. The source mobilities $\mathbf{M}_{s1}$, and $\mathbf{M}_{s2}$ are given by equations (A15) and (A16). The source is considered as a rigid body; in fact, the fundamental resonances of such a block for both longitudinal and flexural waves are out of the frequency range chosen for the simulations [36]. Equations (C4) and (C5) give the mobility matrices $\mathbf{M}_{r1}$ and $\mathbf{M}_{r2}$ for an infinite or a simply supported finite receiver plate. Two external types of excitation act on the complete isolator system: the primary excitation $\mathbf{q}_p$ given by equation (A12) and the flanking excitation $\mathbf{q}_f$ given by equation (C3). The mounting system impedance matrices $\mathbf{Z}_{m1}$ and $\mathbf{Z}_{m2}$ are those of equations (B3) and (B14) and the vector grouping the two control forces $\mathbf{q}_s$ is given by equation (B15).

The junction velocities and force parameters can be derived by using equations (20) and (21) of section 2. In these two equations one makes use of the four matrices given in equations (22)–(25) and the transformation matrix $\mathbf{T}$ given in Appendix D by equation (D2).

4. DYNAMICS OF THE SOURCE/ISOLATOR SYSTEM

In this section the main characteristics of the dynamics for the complete isolating system are introduced. Only the case of an infinite receiver plate is considered at this stage to simplify the discussion. All the simulations in this paper will be carried out in the frequency domain for excitation frequencies between 0 and 1000 Hz.

The power input and power transmitted to the receiver by a "*combined primary excitation*" is considered. The combined primary excitation consists of harmonic axial (F_{zp}) and transverse (F_{yp}) unit forces and harmonic unit torque (T_{xp}) acting on the rigid mass. The dimensions and physical characteristics of the system are given in Table 1.

The power transmission to the receiver for four different thickness of the receiver plate is shown in Figure 3. In the case in which the receiver is very thick (100 mm), the presence of three resonances around 10 Hz and another resonance at 500 Hz is shown in Figure 3(a). The first three resonances correspond to the modes related to the oscillations of the source when the mounts behave as simple springs reacting to axial and transverse forces and to the bending moment. These three modes will be called "*rigid body modes*". Because the receiver is very thick, the dynamics of the system for these modes is quite similar to those of a system with a fixed receiver. It is thus possible to compare the resonances obtained with the simulations by using simple formulae for one-degree-of-freedom systems [29, 30].

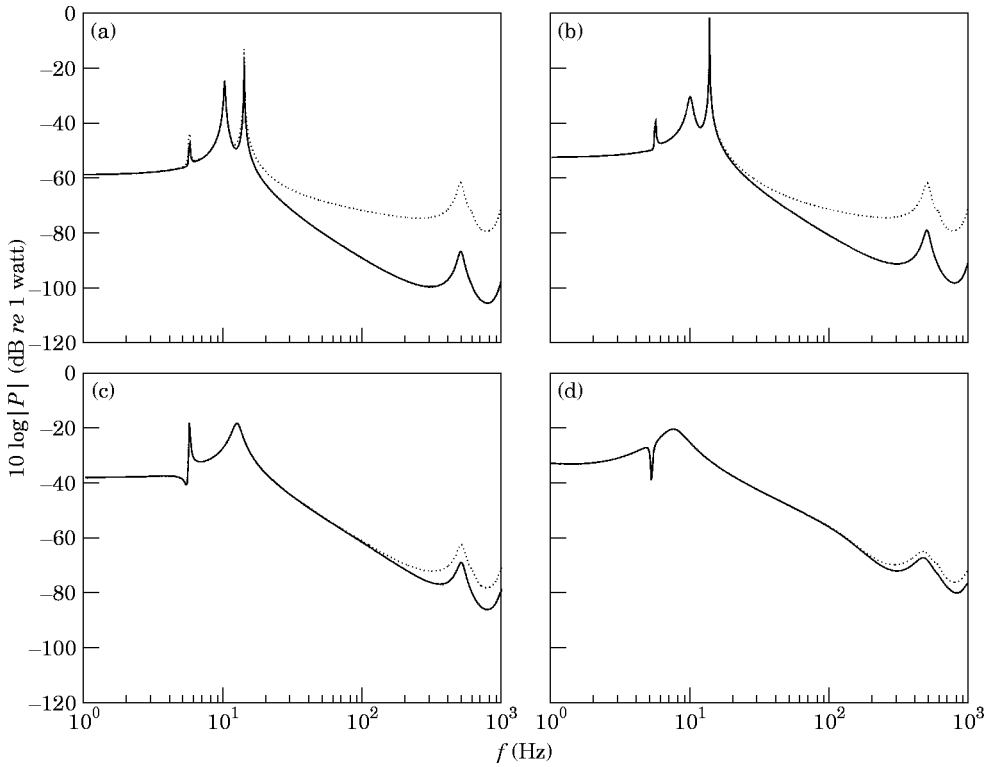

Figure 3. The power input to the source (.....) and to the receiver (——) considering a combined primary excitation (i.e., axial F_{zp} and transverse F_{yp} unit forces and unitary torque T_{xp}) acting at the source. (a) $s = 100$ mm; (b) $s = 50$ mm; (c) $s = 10$ mm; (d) $s = 5$ mm.

These three natural frequencies correspond to a transverse mode, an axial mode, and a pitch mode. As shown in Figure 4, the transverse mode is characterized by two types of motion: the main transverse oscillation and a smaller pitching induced by the bending stress of the mount. The axial mode is given by a pure axial oscillation while the pitch mode is composed of the dominating pitching and a smaller transverse oscillation due, also in this case, to the bending stress induced on the mount. The fundamental natural frequencies of these modes can be estimated by considering the mounts as simple lumped springs and the receiver junctions as fixed points. The transverse mode can be considered as that of a mass connected with two springs reacting to the transverse force induced by the oscillation of the mass. The transverse stiffness of the mounts k_t was derived by assuming the mounts to be rods having a ring cross sectional area. Therefore, $k_t = 12EI_x/h^3$ [30]. So the natural frequency of the transverse mode is given by

$$f_t = (1/2\pi)\sqrt{2k_t/m} = 5{\cdot}9 \text{ Hz}. \tag{33}$$

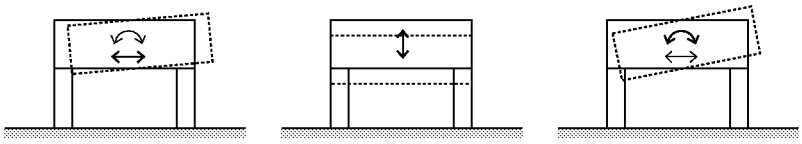

Figure 4. The rigid modes of the complete isolating system for a blocked receiver.

TABLE 2

Natural frequencies of the longitudinal (f_l) and flexural (f_f) modes considering two boundary conditions: both ends clamped (c–c) *and one end clamped and the other free* (c–f)

n	f_l(c–c) (Hz)	f_f(c–c) (Hz)	f_f(c–f) (Hz)
1	500	569·9	93·3
2	1000	1644·0	586·8
3	1500	3222·4	1644·0
4	2000	5326·8	3222·4

The axial normal mode is equivalent to that of a mass connected with two equal springs in parallel reacting to the axial force of the mass. Therefore, upon considering the axial stiffness k_a of a rod having a ring cross sectional area, $k_a = EA/h$ [30], the natural frequency is given by

$$f_a = (1/2\pi)\sqrt{2k_a/m} = 10{\cdot}1 \text{ Hz} \tag{34}$$

The pitch mode can be considered in a first approximation as a mass swinging on two springs reacting with their axial stiffness k_a. Such axial reaction of the two mounts produces two forces acting in opposition on the rigid mass. This pair of forces has an amplitude of $F = 1/2k_a r \sin\theta$, where r is the distance between the two mounts and θ is the angle representing the amplitude of the pitching oscillation of the mass. For small oscillations it can be assumed that $\sin\theta = \theta$, and therefore this pair of forces produces a moment $M = 1/2k_a\, r^2\theta$ acting on the rigid mass. Thus the rotational stiffness associated with the pitching oscillation is given by $k_p = M/\theta = 1/2k_a r^2$ and then the natural frequency is given by

$$f_p = (1/2\pi)\sqrt{k_p/I_G} = 13{\cdot}4 \text{ Hz} \tag{35}$$

where I_G is the moment of inertia with reference to the centre of gravity of the mass and the x-axis. For the system being modelled, the natural frequency of the axial mode will be exactly equal to that in equation (34), while the natural frequency of the transverse and the pitching modes will be given only approximately by equations (33) and (35) since these equations do not take into account the stiffness reacting to the pitching, for the transverse mode, and the stiffness reacting to the transverse oscillations of the mass, for the pitching mode. The effect of the receiver has also been neglected in the above formulation because the plate is so thick.

The resonance at about 500 Hz in Figure 3 is due to the distributed nature of the mounts, in which internal resonances can occur. The mounts of the complete isolating system studied here are excited in such a way that both longitudinal and flexural waves are propagated. The end of the mount connected to the source can be modelled as a clamped end for both longitudinal and flexural waves. The end of the mount connected to the receiver can be considered as clamped for both types of waves when the receiver plate is very thick while when the plate becomes thin the boundary condition for flexural waves changes towards a free end. For such boundary conditions, the natural frequencies of longitudinal and flexural waves are given respectively by the equations [37, 38]

$$f_{ml}(n) = (n/2h)\sqrt{E/\rho}, \qquad f_{mf}(n) = [(\beta_n h)^2/2\pi h^2]\sqrt{EI_x/\rho A}, \tag{36, 37}$$

where n represents the nth natural frequency and $\beta_n h$ is a coefficient that depends on the boundary condition which has been derived from reference [37]. In Table 2 the values of the first four longitudinal and flexural natural frequencies are shown for the mount

dimensions and physical characteristics given in Table 1. These modes will be called "*isolator modes*".

The first natural frequency of the longitudinal wave in the isolator at 500 Hz is shown clearly in Figure 3(a). At around 600 Hz a second peak is also just visible and this is due to the first resonance of a standing flexural wave when the terminations of the mount are clamped (see column 2 of Table 2). Since the thick receiver plate blocks the transverse displacements and the rotations at the mount end this resonance has little effect. The flexural waves are also more heavily damped than longitudinal waves.

From Figures 3(a) it is also possible to estimate the power dissipation of the isolator, by comparing the power input and the power transmitted to the receiver by the primary excitation. The power dissipation clearly increases with the frequency increase.

In Figures 3(b), 3(c) and 3(d) are shown the results for a thinner receiver plate. In this case the receiver plate begins to show the dynamics. At low frequencies both the mounts and the receiver can be modelled as a pair of lumped elements. The receiver effect is purely dissipative for the axial mode, since the input mobility for out-of-plane velocities and forces in a plate is real (see equation C7). On the other hand, for the transverse and pitching modes the behaviour of the receiver is both reactive and dissipative, since the input mobilities for the in-plane velocities and forces, or for rotations and moments, are complex with positive imaginary parts as shown respectively by equations (C6) and (C8). Thus, in principle, both the receiver properties affect the natural frequency of the transverse and the pitching modes and this shows up when the receiver plate becomes thinner (see Figures 3(b), 3(c) and 3(d)). As the plate thickness is reduced, the three rigid body mode resonances become less apparent, until a single flat peak at around 7 Hz is observed for a 5 mm receiver plate, as shown in Figure 3(d). The axial mode is the most affected by the thickness of the receiver plate since it appears as a damper, the resistance of which becomes higher as the plate gets thinner. Two isolator resonances due to flexural waves propagating in the mounts are present, the first is very damped and occurs at around 93 Hz while the second is around 590 Hz. These two resonances agree with the values found by using equation (37) when the mount is assumed to have one end clamped and the other end free (see column 3 of Table 2). The reduction of the plate thickness produces a reduction of the in-plane and angular stiffness of the plate; consequently, the bottom end of the mount is no longer clamped by the reaction of the plate but it behaves more like a free end.

4.1. RESPONSE IN TERMS OF DISPLACEMENTS AND ROTATIONS

In this section, the details of the system vibration are examined for an infinite plate which is 5 mm thick. The frequency response when a single axial harmonic force (F_{zp}) excites the source is considered. This excitation is symmetric with reference to the geometry of the isolator system and the source vibrates only in the axial direction. So, as shown in Figure 5, the source junctions are characterized by axial displacements (w_{s1}, w_{s2}) while the transverse displacements and rotations at the source are zero ($v_{s1} = v_{s2} = 0$, $\theta_{xs1} = \theta_{xs2} = 0$). Although the source moves only in the axial direction, the mounts and the receiver plate are characterized by both longitudinal (longitudinal and shear motion in the plate) and flexural waves. This is because the propagation of axial waves in the mounts generates flexural vibration on the plate when scattered at the receiver junctions and as a consequence of the propagation of these flexural waves from one junction to the other, the receiver junctions vibrate with both out-of-plane displacements (w_{r1}, w_{r2}) and rotations (θ_{xr1}, θ_{xr2}) as shown in Figures 5 and 7. The rotations at the two receiver junctions have the same amplitude but vibrate out of phase. The flexural vibration of the receiver plate generates flexural waves in the mounts. These flexural waves are then scattered at the receiver

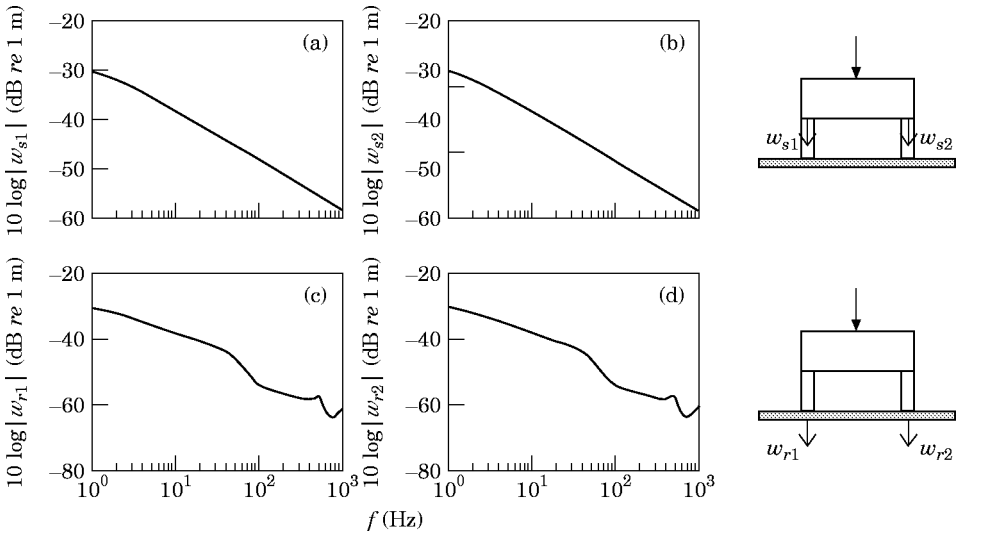

Figure 5. The source axial and receiver out-of-plane displacements when an axial force excites the source and an infinite receiver plate 5 mm thick is considered. (a) Source mount no. 1; (b) source mount no. 2; (c) receiver mount no. 1; (d) receiver mount no. 2.

junctions, inducing in-plane longitudinal and shear waves into the plate. Thus, the receiver junctions also vibrate in the transverse directions, as shown in Figure 6. However, these transverse vibrations have relatively small amplitude when compared to the axial vibration, and this is because the longitudinal and shear waves are characterized by a higher specific impedance than the flexural waves.

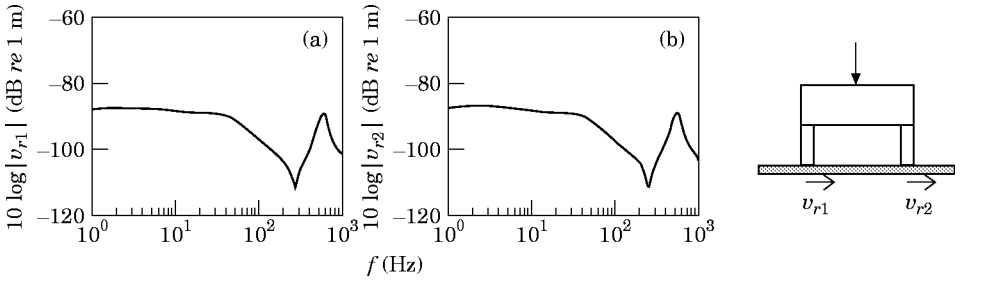

Figure 6. The receiver in-plane displacements when an axial force excites the source and an infinite receiver plate 5 mm thick is considered. (a) Receiver mount no. 1; (b) receiver mount no. 2.

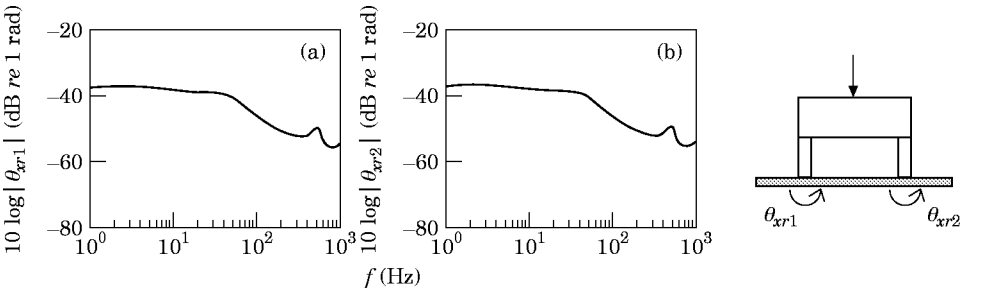

Figure 7. The receiver rotation when an axial force excites the source and an infinite receiver plate 5 mm thick is considered. (a) Receiver mount no. 1; (b) receiver mount no. 2.

The frequency responses of Figure 5 show the isolator resonance due to longitudinal waves in the mounts at 500 Hz, while in Figures 6 and 7 is shown the resonance at 586·8 Hz due to standing flexural waves in the mounts. The first resonance due to standing flexural waves and the natural frequency of the rigid body mode are not visible. The transverse and the pitch rigid body modes are not excited by the primary axial force (F_{zp}) and neither the axial rigid body mode not the first isolator mode are visible because of the high damping effect produced by the infinite receiver plate.

5. POWER TRANSMISSION TO THE RECEIVER

In this section the power transmission to an infinite or a finite plate receiver is investigated. The system studied has the dimensions and the physical characteristics of Table 1 and a 5 mm thick plate is considered. Two different types of excitation are examined: first, a single harmonic *axial unit force* (F_{zp}); and second, a *combined primary excitation* composed of harmonic axial (F_{zp}) and transverse (F_{yp}) unit forces and harmonic unit torque (T_{xp}).

5.1. SYSTEM HAVING AN INFINITE RECEIVER

In Figure 8 is shown the power input into an infinite 5 mm receiver plate and the input power from the primary excitation when an axial force excites the system. The shape of the frequency distribution of power transmission is similar to the frequency response of out-of-plane displacements at the receiver junctions shown in Figure 5. The isolator resonance at 500 Hz due to longitudinal waves is visible, while the axial rigid body mode resonance is very damped and is not visible. The fact that the power spectrum is similar to the frequency response of out-of-plane displacement suggests that the power transmission to the receiver is due mainly to the out-of-plane velocities and forces in this case.

In Figure 9 is shown the power transmission to the receiver and the contribution of each degree of freedom to the power transmission, this confirms that the out-of-plane displacement is by far the most important component in this case, as expected. The axial power is almost equal to the total power transmitted to the receiver in this case (in Figure 9 the thick line, representing total power, hides the thin line representing the axial component

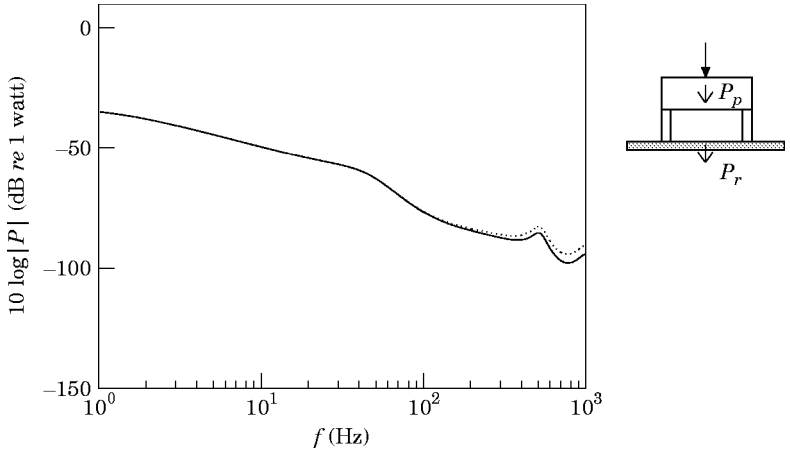

Figure 8. The power input into the source (.....) and transmitted to an infinite plate (——) by an axial primary force.

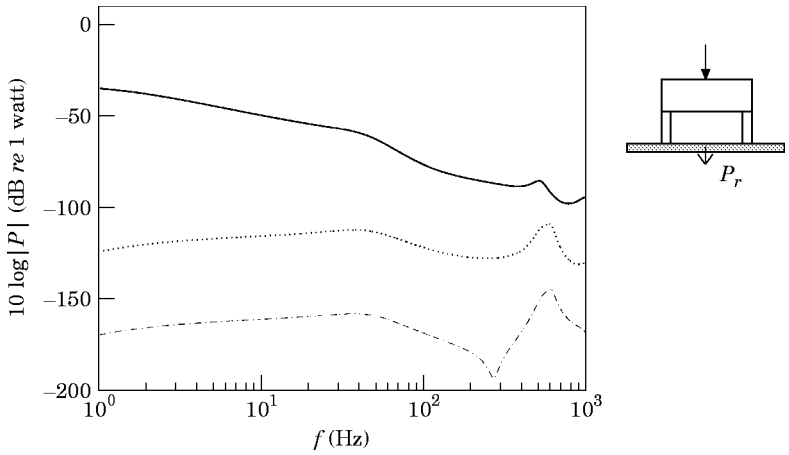

Figure 9. The power transmitted to an infinite plate by an axial primary force. ——, Total power; ——, axial power (coincident with ——); ……, angular power; – · – · –, transverse power.

of power). The angular component of power is much lower than the axial power component transmitted to the receiver but becomes more important as the frequency increases. This agrees with other research [18–22] into the power transmitted to a structure by a force or by a moment. Finally, the transverse component of power transmitted to the receiver is very small compared with the two other components in this case.

The second example considered is for a combined primary excitation acting on the same structure. In Figure 10 is shown the total power input and transmitted to the receiver by the primary source and in Figure 11 is shown the power transmission to the receiver associated with the three degrees of freedom of the system. The three resonances of the rigid body modes are hidden by a single flat peak at around 7 Hz. In Figure 11 it is shown that the total power transmission to the receiver is to a great extent still due to the axial component. The angular component of power is more important in this case than in the previous one, but is still about 20 dB lower than the axial power component. The transverse component of power transmitted to the receiver is still very small at low frequencies, even in this case in which the source is excited by a transverse force. At higher

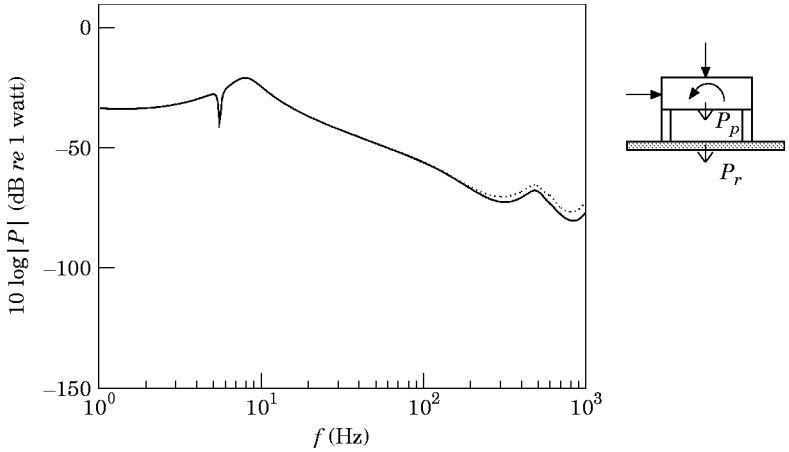

Figure 10. The power input into the source (…….) and transmitted to an infinite plate (——) by a combined primary excitation.

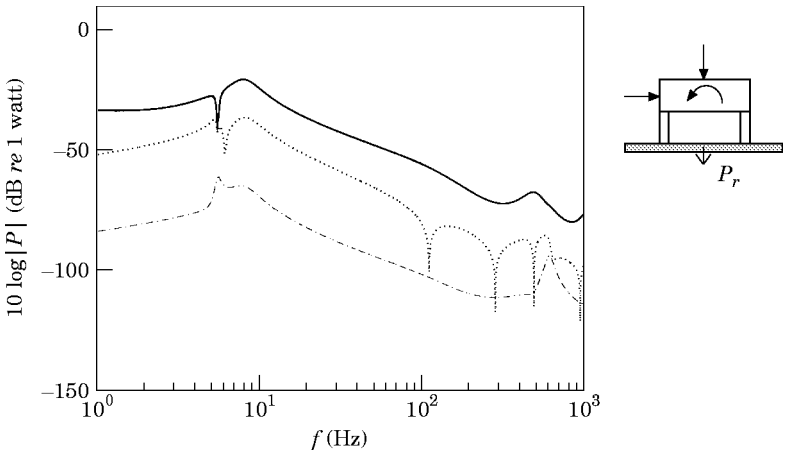

Figure 11. The power transmitted to an infinite plate by a combined primary excitation. ——, Total power; ——, axial power (coincident with ——); ....., angular power; – · – · –, transverse power.

frequencies, however, the transverse component of power does have a similar magnitude to the angular power component, and the flexural isolator resonance at about 600 Hz appears to excite the in-plane motion particularly effectively.

5.2. SYSTEM HAVING A FINITE RECEIVER

The study of power transmission by an isolator to a finite receiver has been investigated by modelling the receiver structure as a simply supported plate. A 5 mm thick aluminium rectangular plate of dimensions 1 m × 1·5 m has been considered. The natural frequencies of the first 126 flexural modes of this plate are listed in Table 3, and all of them have been taken into account in the modal summation for the response. The first modes of in-plane longitudinal or shear waves occur at a frequency higher than 1000 Hz; in the frequency range examined in this paper, the plate thus acts as a spring when excited by in-plane forces. The flexural modes of the finite plate will be called "*receiver modes*" and will refer

TABLE 3

Natural frequencies of the flexural modes of plate 5 mm *thick* (Hz)

$n\backslash m$	1	2	3	4	5	6	7	8	9
1	17·8	54·7	116·3	202·5	313·4	448·9	609·0	793·7	1003·1
2	34·2	71·2	132·7	219·0	329·8	465·3	625·4	810·1	1019·5
3	61·6	98·5	160·1	246·3	357·2	492·7	652·8	837·5	1046·9
4	99·9	136·8	198·4	284·6	395·5	531·0	691·1	875·8	1085·2
5	149·2	186·1	247·7	333·9	444·8	580·2	740·4	925·1	1134·5
6	209·4	246·3	307·9	394·1	505·0	640·5	800·6	985·3	1194·7
7	280·5	317·5	379·1	465·3	576·1	711·6	871·7	1065·5	1265·9
8	362·6	399·6	461·2	547·4	658·2	793·7	953·8	1138·6	1348·0
9	455·7	492·7	554·2	640·5	751·3	886·8	1046·9	1231·6	1441·0
10	559·7	596·7	658·2	744·5	855·3	990·8	1150·9	1335·6	1545·0
11	674·7	711·6	773·2	859·4	970·3	1105·7	1265·9	1450·6	1660·0
12	800·6	837·5	899·1	985·3	1096·2	1231·6	1391·8	1576·5	1785·9
13	937·4	974·4	1035·9	1122·2	1233·0	1368·5	1528·6	1713·3	1922·7
14	1085·2	1122·2	1183·7	1270·0	1380·8	1516·3	1676·4	1861·1	2070·5

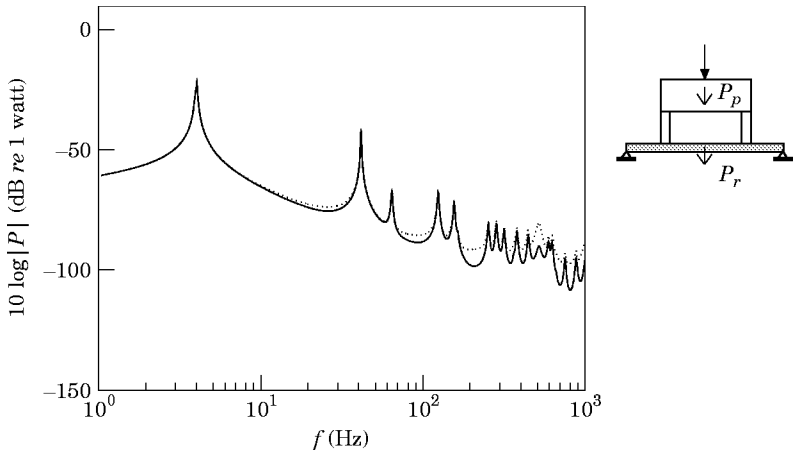

Figure 12. The power input into the source (.....) and transmitted to a finite plate (——) by an axial primary force.

only to flexural vibration of the plate. The simulations refer to a lightly damped plate since the loss factor was assumed to be $\eta = 0{\cdot}02$.

The response of the system to an axial force exciting the source is considered first. In Figure 12 is shown the power input into the system and the power transmitted to the receiver by the primary source. A Comparison of this plot with Figure 8 shows the main differences between a finite receiver and an infinite receiver.

The resonance of the axial rigid body mode is now characterized by a sharp peak at about 4 Hz since the damping effect of the receiving structure is now less effective than in an infinite plate. The shift in frequency (from 6 Hz on an infinite plate) is due to the finite plate receiver reacting elastically to out-of-plane displacements† and so the axial normal mode is now due to the mount stiffness k_{am} in series with the receiver stiffness k_{ar}. Since the mount stiffness of the isolator considered here is the same as those considered before, the total stiffness of the mounts and the receiver connected in series ($k_a = k_{am}k_{ar}/k_{am} + k_{ar}$) is smaller than the stiffness of the mounts alone and then the natural frequency of the axial rigid body mode becomes smaller. At frequencies above the rigid body resonances a large number of peaks characterize the frequency distribution of the power transmitted and the three isolator resonances are now mixed with the resonances of the receiver plate.

Upon comparing Figures 8 and 12 at frequencies above the band of the resonances of the isolator rigid body modes, it is interesting to note that the frequency distribution of the power transmitted to an infinite plate can be considered as the mean value of the power transmitted to a finite plate. The results shown by Pinnington and White in reference [16] can thus be extended to a multi-mount and a multi-directional vibration transmission.

In Figure 13 is shown the power transmission to the receiver through each degree of freedom. The axial power is again almost equal to the total power transmitted to the receiver. In this case, however, the in-plane and angular components of the power are almost equal at low frequencies, although the angular component again becomes more important as the frequency rises.

† The input mobility for out-of-plane velocity and force on a finite plate (equation (C30)) is a complex number with a positive imaginary part indicating a stiffness reaction, whereas the input mobility for out-of-plane velocity and force on an infinite plate (equation (C7)) is a real number indicating only a dissipative effect.

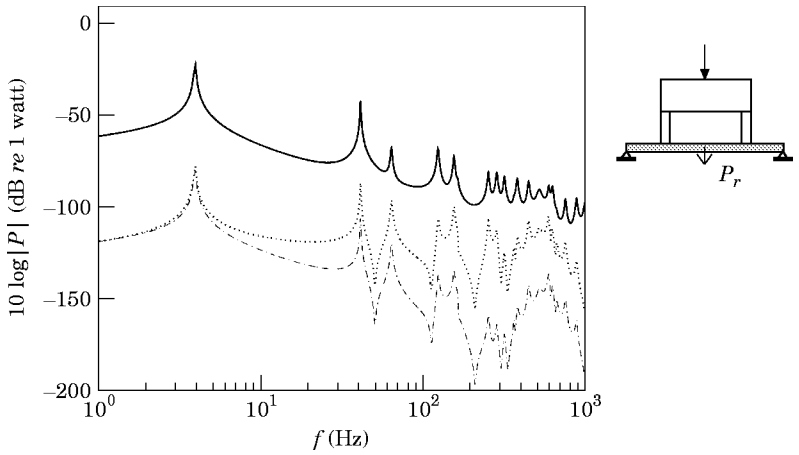

Figure 13. The power transmitted to a finite plate by an axial primary force. ——, Total power; ——, axial power (coincident with ——); ……., angular power, – · – · –, transverse power.

The second case considered is shown in Figures 14 and 15 and is for the example of a combined primary excitation on the source. In this case all three resonances of the rigid body modes are present. The resonance frequencies of the transverse and pitching rigid body modes are also slightly different from those obtained with the infinite receiver plate. The reason for this is again related to the stiffness reaction of the plate. In Figure 15 is shown the power transmission to the receiver through each degree of freedom. In this case the in-plane component of power is even less significant than for axial forcing. The angular power component is particularly significant now, being only about 20 dB lower than the axial power component at higher frequencies.

The plots presented in this and previous sections give a detailed "picture" of the main phenomena in the power transmission to a finite or infinite receiver, respectively. The overall outcome of such results can be summarized by considering the "*efficiency ratio*" of power transmission. This parameter was used by Pan *et al*. [28] and Jenkins *et al*. [39] to describe the vibration of an isolating system similar to the one considered here. The efficiency ratio can be defined as the ratio of the power transmitted to the receiver by an

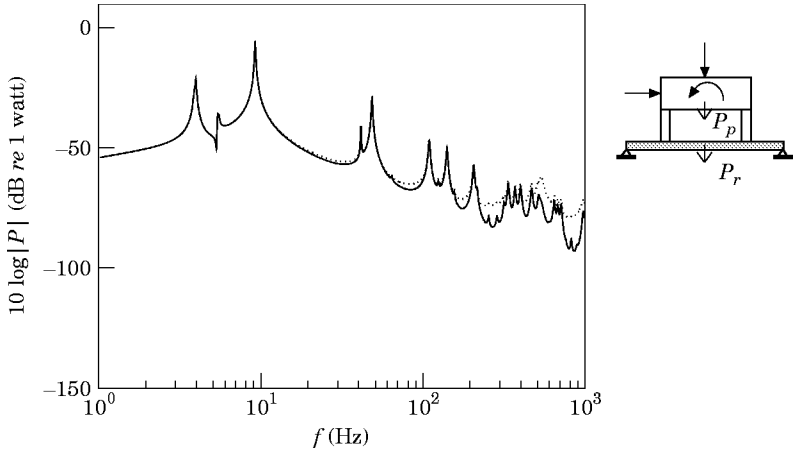

Figure 14. The power input into the source (…….) and transmitted to a finite plate (——) by a combined primary excitation.

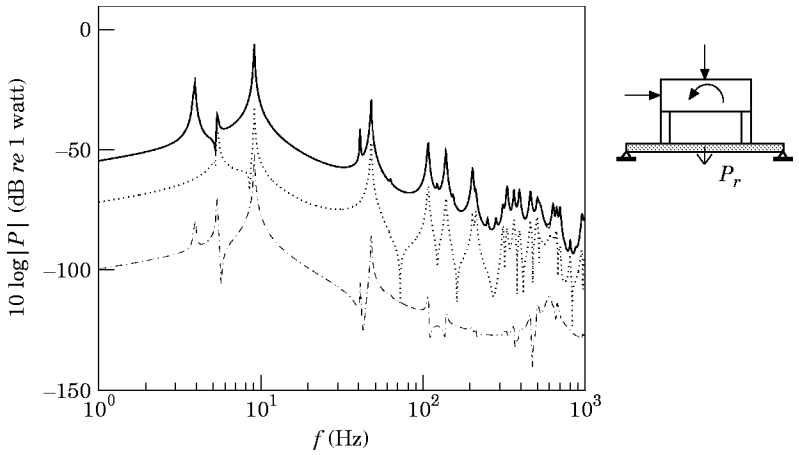

Figure 15. The power transmitted to a finite plate by a combined primary excitation. ——, Total power; ——, axial power (coincident with ——); ……., angular power; – · – · –, transverse power.

isolator with rigid mounts and the power transmitted to the receiver by an isolator with a flexible mounts:

$$E = P_t(\text{rigid mounts})/P_t \text{ (flexible mounts)}. \tag{38}$$

When the efficiency ratio is lower than one, the isolation system performs poorly and a larger quantity of power is transmitted to the receiver than in the case of a rigid link of the source to the receiver.

In Figure 16 is shown the frequency distribution of the efficiency ratio considering the isolator with an infinite or a finite receiver plate. This plot clearly shows that the modal behaviour of the finite receiver plate greatly affects the isolation performance which can be poor at receiver resonance frequencies below 200 Hz, while in the case of an infinite plate the isolation system gives an efficiency ratio greater than one for all frequencies above 20 Hz.

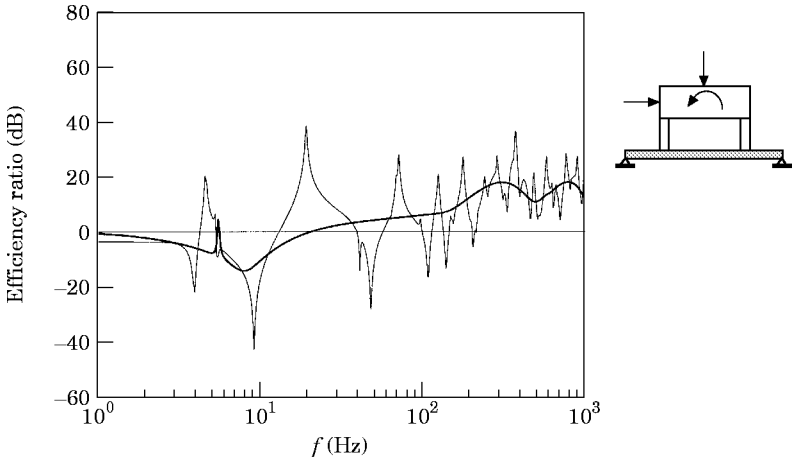

Figure 16. The efficiency of power transmission when an infinite plate (——) or a finite plate (——) is considered and the combined primary excitation acts on the source.

7. CONCLUSIONS

This study is part of an investigation of the effectiveness of active mounts. In this paper a preparatory study has been presented of the mechanism of structural vibration transmission of only a passive isolator.

The system considered comprised a source, free to vibrate in various ways, connected to a flexible receiver by several distributed active mounts. Particular attention was devoted to the study of the multi-mount and multi-directional vibration transmission to a flexible body through distributed passive mounts.

The system was modelled by using a matrix approach with three components: the source, the mounting system and the receiver. The dynamics of each component have been described by using input and transfer mobility terms. The source was modelled as a block mass. The active mounts were modelled as a ring of rubber reacting to axial and transverse displacements and to rotations, and had two opposite axial control forces acting at the mounts ends. Finally, a thin plate receiver in which in-plane longitudinal and shear waves and out-of-plane flexural waves can propagate was considered. The receiver plate was considered to be either infinite, or finite with simply supported boundary conditions at the edges.

A detailed formulation for the mobility or impedance terms for the source, for the mounts and for the receiver is reported in the Appendices. Particular attention has been devoted to the notation used, since even though many of the required terms were derived some time ago, it is still difficult to find references in which a complete and consistent set of mobility or impedance terms is given.

The vibration transmission to the receiver has been quantified by using structural power since this single parameter can be used to describe the dynamics of the system in a consistent manner. The power transmitted to the receiver does not only give a measure of the vibration in the receiving structure but also gives the estimate of noise radiation that in many applications is the real target of the vibration isolation.

The simulations showed that when considering an infinite or a finite receiver plate the frequency distribution of the power transmission is characterized by three peaks at low frequencies related to the natural frequencies of the transverse, axial and pitch rigid body modes of the isolator, all of which are capable of transmitting a large quantity of power to the receiver. At higher frequencies, peaks due to the resonances of the distributed mounts occur, but these peaks are mixed up with many others when a finite receiver is considered since the normal modes of the receiver also strongly affect the power transmission.

It has been shown that power transmission occurs mainly through the axial velocities and force components and the power transmitted through angular velocities and moments increases as the frequency rises. On the other hand, the power transmitted through transverse, in-plane, displacements is very small and could be neglected for a purely passive isolator. We shall see, however, that the in-plane displacements become more important when active control is considered [4].

Comparing the results obtained for the infinite and the finite plate receiver shows that the total power transmitted to the infinite plate can be considered as the mean value of the total power transmitted to a finite receiver plate. This result agrees with the statement of similarity between infinite and finite structures in the vibration isolation presented by other authors [40] and shows that it can be extended to multi-mount and to multi-degree-of-freedom isolators.

ACKNOWLEDGMENTS

The content of this paper is part of a Brite-Euram project supported by the EC under the contract BREU 7228 ASPEN, "Active Control of Structured Vibration Using Power Transmission Methods".

REFERENCES

1. A. H. von Flotow 1988 *Proceedings of the 27th Conference on Decision and Control*, *Austin*, *Texas*, 2029–2033. An expository overview of active control of machinery mounts.
2. D. Karnopp 1995 *Transactions of the American Society of Mechanical Engineers* **117**, 177–185. Active and semi-active vibration isolation.
3. S. J. Elliott and P. A. Nelson 1993 (October) *IEEE Signal Processing Magazine*, 12–35, Active noise control.
4. P. Gardonio, S. J. Elliott and R. J. Pinnington 1997 *Journal of Sound and Vibration* **207**, 95–121. Active isolation of structural vibration on a multiple degree-of-freedom system, part II: effectiveness of active control strategies.
5. A. H. von Flotow 1988 in *Springer Series in Computational Mechanics* (S. N. Atluri and A. K. Amos editors). *Large space structures*: *dynamics and control*. Berlin Springer-Verlag; 213–237. The acoustic limit of control of structural dynamics.
6. D. A. Swanson, L. R. Miller and M. A. Norris 1994 *Journal of Aircraft* **31**(1), 188–196. Multidimensional mount effectiveness for vibration isolation.
7. M. A. Sanderson, C. R. Fredo, L. Ivarsson and M. Gillenang 1995 *Proceedings of Inter-Noise* 95, *Newport Beach*, *California*, 1407–1410. Transfer path analysis including internal force and moment strength estimations at vibration isolators.
8. B. A. T. Petersson and B. M. Gibbs 1993 *Journal of Sound and Vibration* **168**, 157–176. Use of the source descriptor concept in studies of multi-point and multi-directional vibrational sources.
9. H. G. D. Goyder and R. G. White 1980 *Journal of Sound and Vibration* **68**, 59–75. Vibrational power flow from machines into built-up structures, part I: introduction and approximate analyses of beam and plate-like foundations.
10. H. G. D. Goyder and R. G. White 1980 *Journal of Sound and Vibration* **68**, 77–96. Vibrational power flow from machines into built-up structures, part II: wave propagation and power flow in beam-stiffened plates.
11. H. G. D. Goyder and R. G. White 1980 *Journal of Sound and Vibration* **68**, 97–117. Vibrational power flow from machines into built-up structures, part III: power flow through isolation system.
12. D. U. Noiseux 1970 *Journal of the Acoustical Society of America* **47**(2), 238–247. Measurement of power flow in uniform beams and plates.
13. G. Pavic 1976 *Journal of Sound and Vibration* **49**, 221–230. Measurement of structure borne wave intensity, part I: formulation of the method.
14. J. W. Verheij 1980 *Journal of Sound and Vibration* **70**, 133–139. Cross spectral density methods for measuring structure borne power flow on beams and pipes.
15. E. G. Williams, H. D. Dardy and R. G. Fink 1985 *Journal of the Acoustical Society of America* **78**(6), 2061–2068. A technique for measurement of structure-borne intensity in plates.
16. R. J. Pinnington and R. G. White 1980 *Journal of Sound and Vibration* **75**, 179–197. Power flow through machine isolators to resonant and non-resonant beams.
17. R. J. Pinnington 1987 *Journal of Sound and Vibration* **118**, 515–530. Vibrational power transmission to a seating of a vibration isolated motor.
18. B. A. T. Petersson 1993 *Journal of Sound and Vibration* **160**, 43–66. Structural acoustic power transmission by point moment and force excitation, part I: beam- and frame-like structures.
19. B. A. T. Petersson 1993 *Journal of Sound and Vibration* **160**, 67–91. Structural acoustic power transmission by point moment and force excitation, part II: plate-like structures.
20. Y. K. Koh and R. G. White 1996 *Journal of Sound and Vibration* **196**, 469–493. Analysis and control of vibrational power transmission to machinery supporting structures subjected to a multi-excitation system, part I: driving point mobility matrix of beams and rectangular plates.
21. Y. K. Koh and R. G. White 1996 *Journal of Sound and Vibration* **196**, 495–508. Analysis and control of vibrational power transmission to machinery supporting structures subjected to a multi-excitation system, part II vibrational power analysis and control scheme.

22. Y. K. Koh and R. G. White 1996 *Journal of Sound and Vibration* **196**, 509–522. Analysis and control of vibrational power transmission to machinery supporting structures subjected to a multi-excitation system, part III: vibrational power cancellation and control experiments.
23. T. E. Rook and R. Singh 1995 *Journal of the Acoustical Society of America* **97**(5), 2882–2891. Power flow through multidimensional compliant joints using mobility and modal approaches.
24. J. E. Farstad and R. Singh 1995 *Journal of the Acoustical Society of America* **97**(5), 2855–2865. Structurally transmitted dynamic power in discretely joined damped component assemblies.
25. J. M. Mondot and B. Petersson 1987 *Journal of Sound and Vibration* **114**, 507–518. Characterization of structure-borne sound sources: the source descriptor and the coupling function.
26. A. T. Moorhouse and B. M. Gibbs 1993 *Journal of Sound and Vibration* **167**, 223–237. Prediction of the structure-borne noise emission of machines: development of a methodology.
27. A. Moorhouse and B. B. Gibbs 1995 *Acoustic Bulletin November/December* 1995, 21–26. Structure-borne sound—the unheard acoustic.
28. J. Pan, J. Pan and C. H. Hansen 1992 *Journal of the Acoustical Society of America* **92**(2), 895–907. Total power flow from a vibrating rigid body to a thin panel through multiple elastic mounts.
29. C. M. Harris 1961 *Shock and Vibration Handbook*. New York: McGraw-Hill.
30. W. T. Thomson 1981 *Theory of Vibration* Englewood Cliffs. New Jersey: Prentice-Hall.
31. E. J. Skudrzyk 1958 *Journal of the Acoustical Society of America* **30**(12), 1140–1152. Vibrations of a system with a finite or an infinite number of resonances.
32. E. J. Skudrzyk 1959 *Journal of the Acoustical Society of America* **31**(1), 68–74. Theory of noise and vibration insulation of a system with many resonances.
33. E. E. Ungar and C. W. Dietrich 1966 *Journal of Sound and Vibration* **4**, 224–241. High-frequency vibration isolation.
34. J. I. Soliman and M. G. Hallam 1968 *Journal of Sound and Vibration* **8**, 329–351. Vibration isolation between non-rigid machines and non-rigid foundations.
35. J. H. Gordis, R. L. Bielawa and W. G. Flannelly 1990 *Journal of Sound and Vibration* **150**, 139–158. A general theory for frequency domain structural synthesis.
36. P. Gardonio, S. J. Elliott and R. J. Pinnington 1995 *ISVR Technical Memorandum No*. 765, *University of Southampton*. Active isolation of multiple-degree-of-freedom vibration transmission between a source and a receiver.
37. K. F. Graff 1975 *Wave Motion in Elastic Solids*. Oxford University Press.
38. L. Cremer, M. Heckl and E. E. Ungar 1988 *Structure-Borne Sound* (second edition). Berlin; Springer-Verlag.
39. M. D. Jenkins, P. A. Nelson, R. J. Pinnington and S. J. Elliott 1991 *Journal of Sound and Vibration* **166**, 117–140. Active isolation of periodic machinery vibrations.
40. E. J. Skudrzyk 1980 *Journal of the Acoustical Society of America* **67**(4), 1105–1135. The mean-value method of predicting the dynamic response of complex vibrators.
41. R. E. D. Bishop and D. C. Johnson 1960 *The Mechanics of Vibrations*. London: Cambridge University Press.
42. R. C. N. Leung and R. J. Pinnington 1986 *Journal of Sound and Vibration* **111**, 125–129. Point inertance of an infinite plate with respect to a force acting in its plane.
43. S. Ljunggren 1984 *Journal of Sound and Vibration* **100**, 309–320. Transmission of structure-borne sound from a beam into an infinite plate.
44. I. Dyer 1960 *Journal of the Acoustical Society of America* **32**(10), 1290–1297. Moment impedance of plates.
45. R. J. Pinnington 1988 *ISVR Technical Report No* 162, *University of Southampton*. Approximate mobilities of built-up structures.
46. S. Ljunggren 1984 *Journal of Sound and Vibration* **93**, 161–187. Generation of waves in an elastic plate by a torsional moment and a horizontal force.
47. S. Ljunggren 1983 *Journal of Sound and Vibration* **90**, 559–584. Generation of waves in an elastic plate by a vertical force and by a moment in the vertical plane.
48. O. Bardou, P. Gardonio, S. J. Elliott and R. J. Pinnington. *Journal of Sound and Vibration*. (accepted for publication) Active power minimization and power absorption in a plate with force and moment excitation.
49. W. Soedel 1993 *Vibrations of Shells and Plates* (second edition). New York: Marcel Dekker.
50. Lord Rayleigh 1984 *The Theory of Sound* (two volumes). New York: Dover.

APPENDIX A: SOURCE DYNAMICS

Practical applications of complete isolating systems often involve systems having a source of vibration that can be modelled as a rigid mass on which act external forces and moments that represent the source excitation. When more than one mount is attached to the source then the mobility matrices of such subsystems become quite involved. In this Appendix, the matrix formulation is derived for a source modelled as a rigid mass free to vibrate in the y–z plane and excited by forces and a moment acting in the same plane. Two mounts, reacting to axial (z-direction), and transverse (y-direction) displacements and to rotation (θ_x-direction), are connected to the source. As shown in Figure A1, the primary excitation is divided into three components acting on the centre of gravity of the mass (N_{yG}, N_{zG}, M_{xG}); Figure A1 also shows the displacement and force parameters for the two junctions where the source is connected to the mounts.

With reference to the source vectors notation introduced in section 2 for this particular case, the source velocity and force vectors are given by the following set of parameters:

$$\mathbf{v}_s = \begin{Bmatrix} \dot{v}_{s1} \\ \dot{w}_{s1} \\ \dot{\theta}_{xs1} \\ \dot{v}_{s2} \\ \dot{w}_{s2} \\ \dot{\theta}_{xs2} \end{Bmatrix} \qquad \mathbf{f}_s = \begin{Bmatrix} N_{ys1} \\ N_{zs1} \\ M_{xs1} \\ N_{ys2} \\ N_{zs2} \\ M_{xs2} \end{Bmatrix}. \tag{A1, A2}$$

To describe the block mass dynamics with a matrix approach it is convenient to use two new vectors giving the linear–angular velocities and the force–moment parameters at the block mass centre of gravity position, as shown in Figure A1:

$$\mathbf{v}_G = \begin{Bmatrix} \dot{v}_G \\ \dot{w}_G \\ \dot{\theta}_{xG} \end{Bmatrix}, \qquad \mathbf{f}_G = \begin{Bmatrix} N_{yG} \\ N_{zG} \\ M_{xG} \end{Bmatrix}. \tag{A3, A4}$$

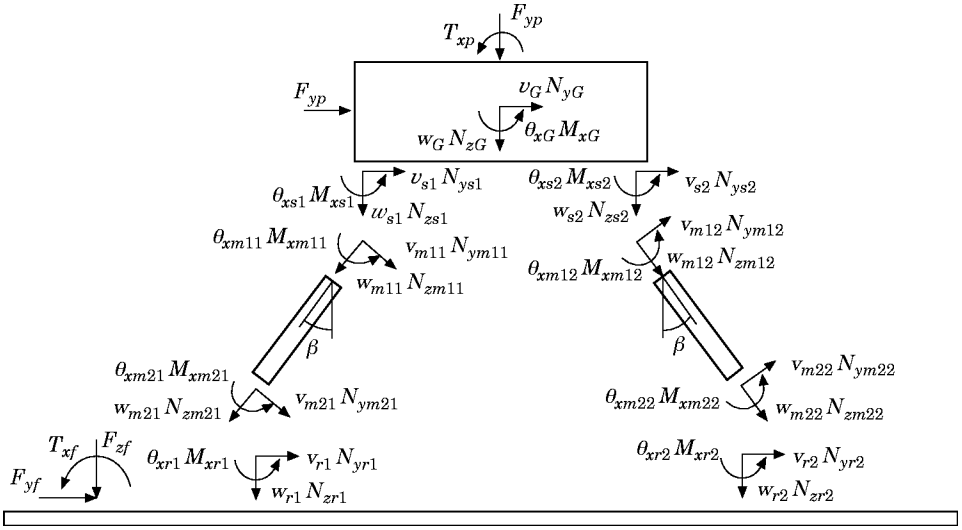

Figure A1. The scheme with the junction parameters of the complete isolating system.

With the block mass considered as a rigid body, for small oscillations these two vectors are related to the source vectors by

$$\mathbf{v}_s = \mathbf{V}_s \mathbf{v}_G, \qquad \mathbf{f}_G = \mathbf{F}_s \mathbf{f}_s, \tag{A5, A6}$$

where

$$\mathbf{V}_s = \begin{bmatrix} 1 & 0 & 0 \\ 0 & 1 & (l_1 - \phi_e)/2 \\ 0 & 0 & 1 \\ 1 & 0 & 0 \\ 0 & 1 & -(l_1 - \phi_e)/2 \\ 0 & 0 & 1 \end{bmatrix}, \tag{A7}$$

$$\mathbf{F}_s = \begin{bmatrix} 1 & 0 & 0 & 1 & 0 & 0 \\ 0 & 1 & 0 & 0 & 1 & 0 \\ l_2/2 & (l_1 - \phi_e)/2 & 1 & l_2/2 & -(l_1 - \phi_e)/2 & 1 \end{bmatrix}, \tag{A8}$$

in which l_1 and l_2 are the dimensions of the block mass and ϕ_e is the diameter of the suspension cross-section. With reference to the centre of gravity parameters and for a motion with time dependence of the form $\exp(j\omega t)$, the dynamic equilibrium principle [29, 30] can be used to obtain the equations

$$N_{yG} + F_{yp} = m\ddot{v}_G = j\omega m\dot{v}_G, \qquad N_{zG} + F_{zp} = m\ddot{w}_G = j\omega m\dot{w}_G,$$
$$M_{xG} + T_{xp} = I_G\ddot{\theta}_{xG} = j\omega I_G\dot{\theta}_{xG}, \tag{A9}$$

where F_{zp}, F_{yp} and T_{xp} are the three components of the primary source of vibration, and m and I_G represent respectively the source mass and the source moment of inertia with respect to the x-axis. These three equations can be summarized in matrix form as

$$\mathbf{f}_G = \mathbf{L}_G \mathbf{q}_p + \mathbf{H}_G \mathbf{v}_G, \tag{A10}$$

so that

$$\mathbf{v}_G = \mathbf{H}_G^{-1}\mathbf{f}_G - \mathbf{H}_G^{-1}\mathbf{L}_G\mathbf{q}_p, \tag{A11}$$

where

$$\mathbf{q}_p = \begin{Bmatrix} F_{yp} \\ F_{zp} \\ T_{xp} \end{Bmatrix} \tag{A12}$$

is the primary excitation vector and the two matrices $\mathbf{L}_G$ and $\mathbf{H}_G$ have the forms

$$\mathbf{L}_G = \begin{bmatrix} -1 & 0 & 0 \\ 0 & -1 & 0 \\ 0 & 0 & -1 \end{bmatrix}, \qquad \mathbf{H}_G = \begin{bmatrix} j\omega m & 0 & 0 \\ 0 & j\omega m & 0 \\ 0 & 0 & j\omega I_G \end{bmatrix}. \tag{A13, A14}$$

Then, by using equations (A5) and (A6), it is possible to express the dynamics of the system in terms of the junction parameters and the primary excitation vector as shown by equation (9) where, in this case, $\mathbf{M}_{s1}$ and $\mathbf{M}_{s2}$ are given by

$$\mathbf{M}_{s1} = \mathbf{V}_s\mathbf{H}_G^{-1}\mathbf{F}_s, \qquad \mathbf{M}_{s2} = -\mathbf{V}_s\mathbf{H}_G^{-1}\mathbf{L}_G. \tag{A15, A16}$$

This result can be extended to a rigid mass free to oscillate into the space and connected with several mounts by using the same approach.

APPENDIX B: MOUNTING SYSTEM DYNAMICS

The mounts of an isolator system can be studied as one dimensional systems composed of several elements. An active mount is composed of two principal parts: a spring for the passive isolation and the actuator to supply the secondary force. Usually the spring is made up of a ring of rubber while the actuator is a more complicated device that could be designed in several ways [2]. These two components could be connected in parallel or series in such a way to give a soft or hard mount [1, 39].

A general *multi-degree-of-freedom mount* reacts to normal and transverse (in two cross-directions) forces and also reacts to bending moments (in two cross-directions) and to a torsional moment. This paper is concerned with a system that can vibrate in a plane and then excite the mounts with normal and transverse forces and a bending moment; these excitations produce longitudinal and flexural waves propagating in the one-dimensional mount.

In this Appendix the impedance matrices of a pair of mounts reacting to an axial force (N_{zm}), to a transverse force (N_{ym}) and to a bending moment (M_{xm}) are given. The mounts have an actuator which is able to act only in the axial direction. The mounts are considered as a flexible continuous system, having a passive behaviour given by a ring of rubber. The control actuator action is modelled as a pair of opposite forces (F_s) applied to the ends of the mounts, and all the passive effects of the actuating device are neglected.

With reference to the matrix formulation introduced in section 2, the dynamics of the mounting system are given by equation (11). In terms of the notation of Figure A1, the velocity and force vectors of the mounts are given by

$$\mathbf{v}_m = \begin{Bmatrix} \mathbf{v}_{m11} \\ \mathbf{v}_{m12} \\ \mathbf{v}_{m21} \\ \mathbf{v}_{m22} \end{Bmatrix}, \qquad \mathbf{f}_s = \begin{Bmatrix} \mathbf{f}_{m11} \\ \mathbf{f}_{m12} \\ \mathbf{f}_{m21} \\ \mathbf{f}_{m22} \end{Bmatrix}, \tag{B1, B2}$$

where, for example, $\mathbf{v}_{m11} = \{\dot{v}_{m11} \;\; \dot{w}_{m11} \;\; \dot{\theta}_{xm11}\}^{\mathrm{T}}$ and $\mathbf{f}_{m11} = \{N_{ym11} \;\; N_{zm11} \;\; M_{xm11}\}^{\mathrm{T}}$. With the two mounts assumed to be identical, the impedance matrix $\mathbf{Z}_{ml}$ of equation (11) is given by

$$\mathbf{Z}_{m1} = \begin{bmatrix} \mathbf{Z}_{11} & \mathbf{0} & \mathbf{Z}_{12} & \mathbf{0} \\ \mathbf{0} & \mathbf{Z}_{11} & \mathbf{0} & \mathbf{Z}_{12} \\ \mathbf{Z}_{21} & \mathbf{0} & \mathbf{Z}_{22} & \mathbf{0} \\ \mathbf{0} & \mathbf{Z}_{21} & \mathbf{0} & \mathbf{Z}_{22} \end{bmatrix}, \tag{B3}$$

where [37, 38, 41]

$$\mathbf{Z}_{11} = \frac{E}{\mathrm{j}\omega} \begin{bmatrix} \dfrac{I_x k_f^3 (\varphi_3 \varphi_4 - \varphi_2 \varphi_1)}{\varphi_4 \varphi_2 - \varphi_3^2} & 0 & \dfrac{I_x k_f^2 (\varphi_3 \varphi_1 - \varphi_2^2)}{\varphi_4 \varphi_2 - \varphi_3^2} \\ 0 & \dfrac{A k_l \lambda_1}{\lambda_2} & 0 \\ \dfrac{I_x k_f^2 (\varphi_4^2 - \varphi_3 \varphi_1)}{\varphi_4 \varphi_2 - \varphi_3^2} & 0 & \dfrac{I_x k_f (\varphi_4 \varphi_1 - \varphi_3 \varphi_2)}{\varphi_4 \varphi_2 - \varphi_3^2} \end{bmatrix}, \tag{B4}$$

$$\mathbf{Z}_{12} = \frac{E}{\mathrm{j}\omega}\begin{bmatrix} \dfrac{I_x k_f^3 \varphi_2}{\varphi_4 \varphi_2 - \varphi_3^2} & 0 & -\dfrac{I_x k_f^2 \varphi_3}{\varphi_4 \varphi_2 - \varphi_3^2} \\ 0 & -\dfrac{A k_l}{\lambda_2} & 0 \\ \dfrac{I_x k_f^2 \varphi_3}{\varphi_4 \varphi_2 - \varphi_3^2} & 0 & -\dfrac{I_x k_f \varphi_4}{\varphi_4 \varphi_2 - \varphi_3^2} \end{bmatrix}, \tag{B5}$$

$$\mathbf{Z}_{21} = \frac{E}{\mathrm{j}\omega}\begin{bmatrix} \dfrac{I_x k_f^3 \varphi_2}{\varphi_4 \varphi_2 - \varphi_3^2} & 0 & \dfrac{I_x k_f^2 \varphi_3}{\varphi_4 \varphi_2 - \varphi_3^2} \\ 0 & -\dfrac{A k_l}{\lambda_2} & 0 \\ -\dfrac{I_x k_f^2 \varphi_3}{\varphi_4 \varphi_2 - \varphi_3^2} & 0 & -\dfrac{I_x k_f \varphi_4}{\varphi_4 \varphi_2 - \varphi_3^2} \end{bmatrix}, \tag{B6}$$

$$\mathbf{Z}_{22} = \frac{E}{\mathrm{j}\omega}\begin{bmatrix} \dfrac{I_x k_f^3 (\varphi_3 \varphi_4 - \varphi_2 \varphi_1)}{\varphi_4 \varphi_2 - \varphi_3^2} & 0 & -\dfrac{I_x k_f^2 (\varphi_3 \varphi_1 - \varphi_2^2)}{\varphi_4 \varphi_2 - \varphi_3^2} \\ 0 & \dfrac{A k_l \lambda_1}{\lambda_2} & 0 \\ -\dfrac{I_x k_f^2 (\varphi_4^2 - \varphi_3 \varphi_1)}{\varphi_4 \varphi_2 - \varphi_3^2} & 0 & \dfrac{I_x k_f (\varphi_4 \varphi_1 - \varphi_3 \varphi_2)}{\varphi_4 \varphi_2 - \varphi_3^2} \end{bmatrix}, \tag{B7}$$

in which E is the Young's modulus of elasticity, A and I_x are, respectively, the area and the moment of inertia for the cross-section of the mount (with reference to the x-axis), and k_l and k_f are, respectively, the wavenumbers of the quasi-longitudinal and flexural waves in a beam. The damping effect can be introduced by considering a complex wavenumber [38]. The other terms are given by the following expressions [41]:

$$\lambda_1 = \cos k_l h, \qquad \lambda_2 = \sin k_l h, \tag{B8, B9}$$

$$\varphi_1 = \tfrac{1}{2}[\cosh k_f h + \cos k_f h], \qquad \varphi_3 = \tfrac{1}{2}[\cosh k_f h - \cos k_f h], \tag{B10, B11}$$

$$\varphi_2 = \tfrac{1}{2}[\sinh k_f h + \sin k_f h], \qquad \varphi_4 = \tfrac{1}{2}[\sinh k_f h - \sin k_f h], \tag{B12, B13}$$

in which h is the height of the actuator for a single mount. The impedance matrix $\mathbf{Z}_{m2}$ and the control excitation vector in equation (11) have the forms

$$\mathbf{Z}_{m2} = \begin{bmatrix} -\mathbf{T}_1 \\ -\mathbf{T}_2 \\ \mathbf{T}_1 \\ \mathbf{T}_2 \end{bmatrix}, \qquad \mathbf{q}_s = \begin{Bmatrix} F_{s1} \\ F_{s2} \end{Bmatrix}, \tag{B14, B15}$$

where

$$\mathbf{T}_1 = \begin{bmatrix} 1 & 0 \\ 0 & 0 \\ 0 & 0 \end{bmatrix}, \qquad \mathbf{T}_2 = \begin{bmatrix} 0 & 1 \\ 0 & 0 \\ 0 & 0 \end{bmatrix}. \tag{B16, B17}$$

The procedure for determining the impedance matrices, presented above, can be extended to a system having several mounts; moreover, the expression for the impedance matrix $\mathbf{Z}_{ml}$ can be enlarged to the remaining degrees of freedom (u, θ_y, θ_z) in such a way as to include the flexural vibration in the x–z plane and the torsional vibration. The expressions for the point and transfer mobilities for the flexural vibration in the x–z plane are the same as those found in equations (B4)–(B7) for the flexural vibration in the y–z plane, except that the moment of inertia must refer to the y-axis (I_y). Also, the point and transfer impedance terms for the torsional vibration have the same forms as those found for the longitudinal wave but must refer to the torsional stiffness of the beam [41].

APPENDIX C: RECEIVER DYNAMICS

The receiving structure, on which the source of vibration is mounted via a mounting system, can be a general type of continuous flexible structure. For example, the receiving structure of isolators for the engines of cars, ships or aeroplanes is generally a stiffened plate or a stiffened shell, while the structure for isolators for electric motors installed on domestic machines is usually a case.

In this Appendix a simple receiver system is considered. The dynamics of a flat infinite or finite plate are studied, when excited by out-of-plane and in-plane forces and by bending moments. The in-plane forces are assumed to act in the middle of the plate cross-section and thus generate only in-plane longitudinal waves and in-plane shear (transverse) waves, while the out-of-plane force and the flexural moment generate only out-of-plane flexural waves. Longitudinal and shear (transverse) waves are characterized by in-plane displacements $u(x, y)$ and $v(x, y)$, while the flexural wave is characterized by out-of-plane displacements $w(x, y)$ and plate cross-section rotations $\theta_x(x, y)$ and $\theta_y(x, y)$. The formulation reported in this Appendix does not include consideration of the action of a torsional moment which generates shear (transverse) waves. The dynamics of the receiver system is given by equation (10). As shown in Figure 2, the complete isolating system studied in this paper is characterized by a rigid mass connected to the receiver plate through two mounts. The junctions connecting the mounts of the plate and the flanking excitation forces and moment are placed along a line parallel to the y-axis at $x = l_x/2$. As shown in Figure A1, the two mounts excite the plate with a pair of out-of-plane forces N_{zr1} and N_{zr2}, with a pair of in-plane forces N_{yr1} and N_{yr2} and with a pair of moments M_{xr1} and M_{xr2}. The flanking excitation consists of an out-of-plane force F_{zf}, an in-plane force F_{yf} and a torque in the y–z plane, T_{xf}. Therefore, the formulation of the two mobility matrices is simplified since only some of the degrees of freedom at a fixed position of the receiver plate are considered. In fact, with reference to the notation of Figure A1, the receiver velocity, force vector and flanking excitation vector used in equation (10) are given, respectively, by

$$\mathbf{v}_r = \begin{Bmatrix} \dot{v}_{r1} \\ \dot{w}_{r1} \\ \dot{\theta}_{xr1} \\ \dot{v}_{r2} \\ \dot{w}_{r2} \\ \dot{\theta}_{xr2} \end{Bmatrix}, \qquad \mathbf{f}_r = \begin{Bmatrix} N_{yr1} \\ N_{zr1} \\ M_{xr1} \\ N_{yr2} \\ N_{zr2} \\ M_{xr2} \end{Bmatrix}, \qquad \mathbf{q}_f = \begin{Bmatrix} F_{yf} \\ F_{zf} \\ T_{xf} \end{Bmatrix}. \tag{C1–C3}$$

Because only the in-plane force (N_{yr}) produces in-plane vibration (v_r) while only the out-of-plane force (N_{zr}) and the moment (M_{xr}) produce out-of-plane (w_r) and angular (θ_{xr}) vibration, the two mobility matrices $\mathbf{M}_{r1}$ and $\mathbf{M}_{r2}$ of equation (10) are given by

$$\mathbf{M}_{r1} = \begin{bmatrix} m_{vN_y}^{11} & 0 & 0 & m_{vN_y}^{12} & 0 & 0 \\ 0 & m_{wN_z}^{11} & m_{wM_x}^{11} & 0 & m_{wN_z}^{12} & m_{wM_x}^{12} \\ 0 & m_{\theta_x N_z}^{11} & m_{\theta_x M_x}^{11} & 0 & m_{\theta_x N_z}^{12} & m_{\theta_x M_x}^{12} \\ m_{vN_y}^{21} & 0 & 0 & m_{vN_y}^{22} & 0 & 0 \\ 0 & m_{wN_z}^{21} & m_{wM_x}^{21} & 0 & m_{wN_z}^{22} & m_{wM_x}^{22} \\ 0 & m_{\theta_x N_z}^{21} & m_{\theta_x M_x}^{21} & 0 & m_{\theta_x N_z}^{22} & m_{\theta_x M_x}^{22} \end{bmatrix},$$

$$\mathbf{M}_{r2} = \begin{bmatrix} m_{vN_y}^{1p} & 0 & 0 \\ 0 & m_{wN_z}^{1p} & m_{wM_x}^{1p} \\ 0 & m_{\theta_x N_z}^{1p} & m_{\theta_x M_x}^{1p} \\ m_{vN_y}^{2p} & 0 & 0 \\ 0 & m_{wN_z}^{2p} & m_{wM_x}^{2p} \\ 0 & m_{\theta_x N_z}^{2p} & m_{\theta_x M_x}^{2p} \end{bmatrix}, \qquad \text{(C4, C5)}$$

where m^{ij} indicates a point mobility term at the jth junction while the term m^{ik} indicates a transfer mobility term between junction j (where the velocity is evaluated) and junction k (where the excitation is acting). It should be said that equation (C4) refers to any type of plate and when the infinite plate case is considered the point mobility terms $m_{\theta_x N_z}^{ij}$ and $m_{wM_x}^{ij}$ are zero.

The next two sections give general mobility equations for either an infinite or a finite plate. With these formulae it is then possible to derive the mobilities of the two matrices $\mathbf{M}_{r1}$ and $\mathbf{M}_{r2}$.

One of the peculiarities of the formulation reported in the two following sections is the notation used, which has been carefully planned with reference to the matrix model discussed in section 2. In this way the equations presented could be used in any model having plate elements. In Figure C1 is shown the notation used for the in-plane displacements (u and v) and the in-plane forces (N_x and N_y) at two generic points of a plate, while in Figure C2 is shown the notation at two generic points of a plate used for the out-of-plane displacement (w), for the rotation in a general direction in the x–y plane (θ_d), for the out-of-plane force (N_z) and for the moment in a general direction in the x–y plane (M_d). At each of these two points, a local system of reference composed of a right-handed triple of vectors (x, y, z) is defined. The formulation of the transfer mobility terms in an

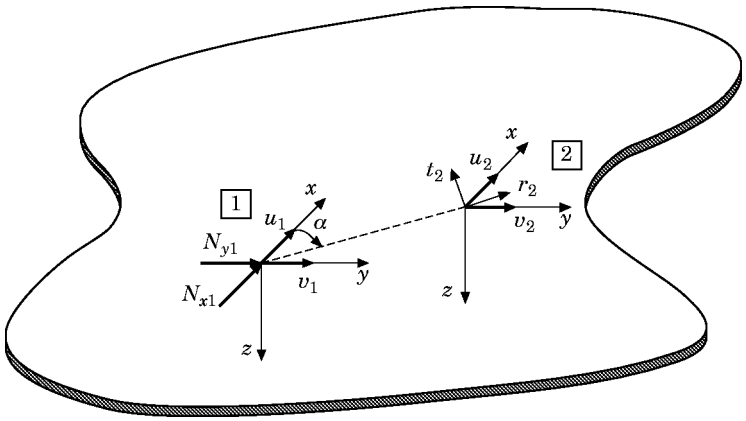

Figure C1. The notation used for the in-plane forces and for the in-plane displacements for two generic points of the receiver plate.

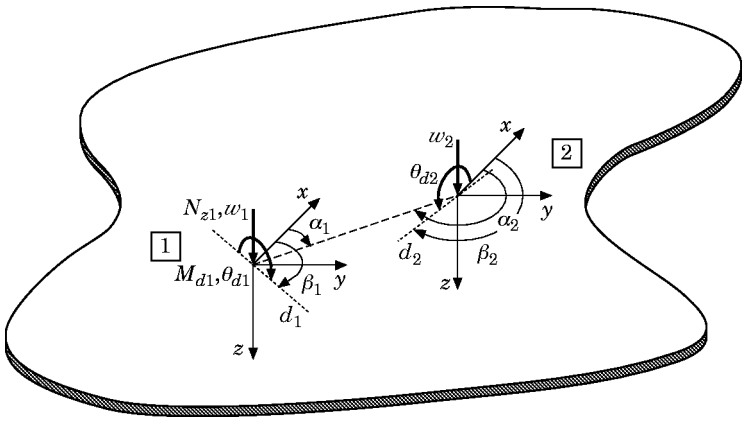

Figure C2. The notation used for the out-of-plane force and moment and for the out-of-plane displacements and rotations for two generic points of the receiver plate.

infinite plate requires knowledge of the angle α, which is defined as the angle between the x-axis and the segment r joining the two points examined. This angle is defined as positive with reference to the right-handed screw rule. For the mobilities involving angular velocities or flexural moments of a second angle β is used and this is defined as the angle between the x-axis and the segment d, as shown in Figure C2.

C1. INFINITE PLATE

In the formulation below, the point mobility for in-plane or out-of-plane forces, and for the moments, contains the local indenter effect, which is the cause of the imaginary parts in the mobility; when the transfer mobilities are considered, however, these local effects can be ignored, and the imaginary parts of the mobilities are due only to the wave propagating effects. The input mobility terms m^{jj} are considered first with reference to position 1. The in-plane velocities $\dot{u}_1$ and $\dot{v}_1$ are related respectively to the in-plane forces N_{x1} and N_{y1} by two mobility terms, one for the longitudinal wave and for the shear (transverse) wave [42, 43]

$$m^{11}_{uNx} = \frac{\dot{u}_{r1}}{N_{xr1}} = m^{11}_{vNy} = \frac{\dot{v}_{r1}}{N_{yr1}} = \frac{\omega}{8D}\left[1 + \frac{\mathrm{j}}{\pi}\ln\left(\frac{\omega_l}{\omega}\right)^2\right] + \frac{\omega}{8S}\left[1 + \frac{\mathrm{j}}{\pi}\ln\left(\frac{\omega_s}{\omega}\right)^2\right], \qquad \text{(C6)}$$

where $D = sE/1 - v^2$ and $S = sG$ are, respectively, the longitudinal and shear stiffness, s is the plate thickness, E is the Young's modulus of elasticity, G is the shear modulus of elasticity and v is the Poisson ratio. $\omega_l = \pi\sqrt{D/4\rho s\phi_e^2}$, $\omega_s = \pi\sqrt{S/4\rho s\phi_e^2}$, ρ is the density and ϕ_e is the diameter of the indenter. The out-of-plane force N_{z1} generates a flexural wave that at position 1 is characterized only by transverse $\dot{w}_1$ velocity. Therefore, the point mobility associated with this excitation is [38]

$$m^{11}_{wNz} = \dot{w}_1/N_{z1} = \omega/8Bk_f^2, \qquad \text{(C7)}$$

where $B = Es^3/12(1 - v^2)$ is the flexural stiffness for the plate and k_f is the wavenumber of flexural waves in the plate. Also, the torques M_{x1} and M_{y1} generate a flexural wave that at position 1 is characterized only by plate angular velocities that are, respectively, $\dot{\theta}_{x1}$ and $\dot{\theta}_{y1}$. The two mobilities are then given by [44, 45]

$$m^{11}_{\theta xMx} = \frac{\dot{\theta}_{x1}}{M_{x1}} = m^{11}_{\theta yMy} = \frac{\dot{\theta}_{y1}}{M_{y1}} = \frac{\omega}{8B(1 + L)}\left[1 + \mathrm{j}\,\frac{4}{\pi}\ln k_f\,\phi_e - \frac{\mathrm{j}8L}{\pi(1 - v)}\left(\frac{s}{\pi\phi_e}\right)^2\right], \qquad \text{(C8)}$$

where L is a parameter which tends to unity for large ϕ_e/s [9]. The transfer mobilities are now examined for the particular case on which the velocities are evaluated at position 2 while the forces or moments are applied at position 1. With reference to the notation introduced in Figure C1, the in-plane forces N_{x2} or N_{y2} produce axial and shear waves that propagate with a typical dipole velocity distribution. The transfer mobilities in polar co-ordinates (r, t) for the in-plane N_{y2} excitation are given by [46]:

$$M^{21}_{rNy} = \frac{\dot{r}_2}{N_{y1}} = \frac{\omega}{4D}\left[\mathrm{H}_0^{(2)}(k_l\, r) - \frac{1}{k_l\, r}\,\mathrm{H}_1^{(2)}(k_l\, r)\right]\sin\alpha + \frac{\omega}{4S}\left[\frac{1}{k_t\, r}\,\mathrm{H}_1^{(2)}(k_t\, r)\right]\sin\alpha, \quad \text{(C9)}$$

$$M^{21}_{tNy} = \frac{\dot{t}_2}{N_{y1}} = \frac{\omega}{4D}\left[\frac{1}{k_l\, r}\,\mathrm{H}_1^{(2)}(k_l\, r)\right]\cos\alpha + \frac{\omega}{4S}\left[\mathrm{H}_0^{(2)}(k_t\, r) + \frac{1}{k_t\, r}\,\mathrm{H}_1^{(2)}(k_t\, r)\right]\cos\alpha, \quad \text{(C10)}$$

where k_l and k_t are, respectively, the wavenumbers of quasi-longitudinal waves and shear waves in the plate. $\mathrm{H}_i^{(2)}$ is the second kind of Hankel function of the ith order. With these two equations it is then possible to derive the two mobility terms m^{21}_{uNy} and m^{21}_{vNy} relating the N_{y1} in-plane force to the in-plane $\dot{u}_2$ and $\dot{v}_2$ velocities. A similar procedure can be used to derive the two mobility terms m^{21}_{uNx} and m^{21}_{vNx} relating the N_{x1} in-plane force to the in-plane $\dot{u}_2$ and $\dot{v}_2$ velocities respectively. If a bending moment M_{d1} and an angular velocity $\dot{\theta}_{d2}$ with general orientation, defined respectively by the angles β_1 and β_2, are considered, the following four transfer mobility terms can be derived [11, 47, 48]:

$$M^{21}_{wNz} = \frac{\dot{w}_2}{N_{z1}} = \frac{\omega}{8Bk_f^2}\left[\mathrm{H}_0^{(2)}(k_f\, r) - \mathrm{j}\,\frac{2}{\pi}\,\mathrm{K}_0(k_f\, r)\right], \quad \text{(C11)}$$

$$M^{21}_{wMd} = \frac{\dot{w}_2}{M_{d1}} = \frac{\omega}{8Bk_f}\left[\mathrm{H}_1^{(2)}(k_f\, r) - \mathrm{j}\,\frac{2}{\pi}\,\mathrm{K}_1(k_f\, r)\right]\cos\varepsilon_1, \quad \text{(C12)}$$

$$M^{21}_{\dot{\theta}dNd} = \frac{\dot{\theta}_{d2}}{N_{z1}} = \frac{\omega}{8Bk_f}\left[\mathrm{H}_1^{(2)}(k_f\, r) - \mathrm{j}\,\frac{2}{\pi}\,\mathrm{K}_1(k_f\, r)\right]\cos\varepsilon_2, \quad \text{(C13)}$$

$$M^{21}_{\dot{\theta}dMd} = \frac{\dot{\theta}_{d2}}{M_{d1}} = \frac{\omega}{8B}\left\{\left[\mathrm{H}_0^{(2)}(k_f\, r) - \frac{1}{k_f\, r}\,\mathrm{H}_1^{(2)}(k_f\, r) + \mathrm{j}\,\frac{2}{\pi}\left(\mathrm{K}_0(k_f\, r) + \frac{1}{k\, r}\,\mathrm{K}_1(k_f\, r)\right)\right]\right.$$

$$\left.\times\cos(\varepsilon_1 - \delta_2)\cos\varepsilon_1 - \frac{1}{k_f\, r}\left[\mathrm{H}_1^{(2)}(k_f\, r) - \mathrm{j}\,\frac{2}{\pi}\,\mathrm{K}_1(k_f\, r)\right]\sin(\varepsilon_1 - \delta_2)\sin\varepsilon_1\right\}. \quad \text{(C14)}$$

Here $\delta_1 = \beta_2 - \beta_1$, $\delta_2 = \beta_1 - \beta_2$, $\varepsilon_1 = \alpha_1 - \beta_1$, $\varepsilon_2 = \alpha_2 - \beta_2$, $\mathrm{H}_i^{(2)}$ is the second kind of Hankel function of the ith order and K_i is the second kind of modified Bessel function of the ith order. If the moment and the angular velocity parameters are aligned, then $\beta_1 = \alpha_1$ or $\beta_1 = \alpha_1 + \pi$ and $\beta_2 = \alpha_2$ or $\beta_2 = \alpha_2 + \pi$. Therefore equation (C14) assumes the following simplified form [48]:

$$Y^{21}_{\dot{\theta}dMd} = \frac{\dot{\theta}_{d2}}{M_{d1}} = \frac{\omega}{8B}\left[\mathrm{H}_0^{(2)}(k_f\, r) - \frac{1}{k_f\, r}\,\mathrm{H}_1^{(2)}(k_f\, r) + \mathrm{j}\,\frac{2}{\pi}\left(\mathrm{K}_0(k_f\, r) + \frac{1}{\mathrm{K}_f\, r}\,\mathrm{K}_1(k_f\, r)\right)\right]. \quad \text{(C15)}$$

By using equation (C12) it is possible to derive the expressions for the mobility terms $m^{21}_{wM_x}$ and $m^{21}_{wM_y}$, while from equation (C13) the mobility terms $m^{21}_{\theta xNz}$ and $m^{21}_{\theta yNz}$ can be derived. Finally, by using equation (C14) the four mobility terms $m^{21}_{\theta xMx}$, $m^{21}_{\theta yMx}$, $m^{21}_{\theta xMy}$ and $m^{21}_{\theta yMy}$ can be evaluated.

C.2. FINITE PLATE

The notation used is the same as shown in Figures C1 and C2, and a main system of reference is considered at the left bottom corner of the plate, as shown in Figure 2. The simply supported boundary condition imposes the following restraints at the edges of the plate:

$$x = 0 \text{ and } x = l_x, \qquad v = w = 0, \qquad \partial^2 v/\partial x^2 = \partial^2 w/\partial x^2 = 0, \qquad \partial u/\partial x = 0,$$

$$y = 0 \text{ and } y = l_y, \qquad u = w = 0, \qquad \partial^2 u/\partial x^2 = \partial^2 w/\partial x^2 = 0, \qquad \partial v/\partial x = 0.$$

When a finite structure is considered, the formulae for the point and transfer mobilities have the same form. Therefore, the following equations are given for transfer mobilities but can equally be applied for point mobilities. The in-plane velocities $\dot{u}_2$ and $\dot{v}_2$ relate, respectively, to the in-plane forces N_{x1} and N_{y1} via two mobility terms, one for the longitudinal wave and one for the shear (transverse) wave [49]:

$$m^{21}_{uNx} = \frac{\dot{u}_2}{N_{x1}} = \mathrm{j}\omega \sum_{m=0}^{\infty}\sum_{n=0}^{\infty} \frac{\lambda^{(x)}_{m,n}(x_2, y_2)\lambda^{(x)}_{m,n}(x_1, y_1)}{\Lambda[\omega^2_{lm,n}(1 + \mathrm{j}\eta) - \omega^2]} + \mathrm{j}\omega \sum_{m=0}^{\infty}\sum_{n=0}^{\infty} \frac{\lambda^{(x)}_{m,n}(x_2, y_2)L^{(x)}_{m,n}(x_1, y_1)}{\Lambda[\omega^2_{sm,n}(1 + \mathrm{j}\eta) - \omega^2]}, \tag{C16}$$

$$m^{21}_{uNy} = \frac{\dot{u}_2}{N_{y1}} = \mathrm{j}\omega \sum_{m=0}^{\infty}\sum_{n=0}^{\infty} \frac{\lambda^{(x)}_{m,n}(x_2, y_2)\lambda^{(y)}_{m,n}(x_1, y_1)}{\Lambda[\omega^2_{lm,n}(1 + \mathrm{j}\eta) - \omega^2]} + \mathrm{j}\omega \sum_{m=0}^{\infty}\sum_{n=0}^{\infty} \frac{\lambda^{(x)}_{m,n}(x_2, y_2)\lambda^{(y)}_{m,n}(x_1, y_1)}{\Lambda[\omega^2_{sm,n}(1 + \mathrm{j}\eta) - \omega^2]}, \tag{C17}$$

$$m^{21}_{vNx} = \frac{\dot{v}_2}{N_{x1}} = \mathrm{j}\omega \sum_{m=0}^{\infty}\sum_{n=0}^{\infty} \frac{\lambda^{(y)}_{m,n}(x_2, y_2)\lambda^{(x)}_{m,n}(x_1, y_1)}{\Lambda[\omega^2_{lm,n}(1 + \mathrm{j}\eta) - \omega^2]} + \mathrm{j}\omega \sum_{m=0}^{\infty}\sum_{n=0}^{\infty} \frac{\lambda^{(y)}_{m,n}(x_2, y_2)\lambda^{(x)}_{m,n}(x_1, y_1)}{\Lambda[\omega^2_{sm,n}(1 + \mathrm{j}\eta) - \omega^2]}, \tag{C18}$$

$$m^{21}_{vNy} = \frac{\dot{v}_2}{N_{y1}} = \mathrm{j}\omega \sum_{m=1}^{\infty}\sum_{n=1}^{\infty} \frac{\lambda^{(y)}_{m,n}(x_2, y_2)\lambda^{(y)}_{l,m}(x_1, y_1)}{\Lambda[\omega^2_{lm,n}(1 + \mathrm{j}\eta) - \omega^2]} + \mathrm{j}\omega \sum_{m=0}^{\infty}\sum_{n=0}^{\infty} \frac{\lambda^{(y)}_{m,n}(x_2, y_2)\lambda^{(y)}_{l,m}(x_1, y_1)}{\Lambda[\omega^2_{sm,n}(1 + \mathrm{j}\eta) - \omega^2]}. \tag{C19}$$

Here $\Lambda = \rho s l_x l_y/2$ is the modal mass, $\omega_{lm,n}$ and $\omega_{sm,n}$ are the m,nth natural frequencies associated, respectively, with the longitudinal and shear waves propagating on the plate, η is the loss factor and $\lambda^{(x)}_{m,n}$, $\lambda^{(y)}_{m,n}$ are the m,nth eigenfunctions [50]:

$$\omega_{lm,n} = \sqrt{\frac{E}{\rho(1-\nu^2)}\left[\left(\frac{m\pi}{l_x}\right)^2 + \left(\frac{n\pi}{l_y}\right)^2\right]}, \qquad \omega_{sm,n} = \sqrt{\frac{G}{\rho}\left[\left(\frac{m\pi}{l_x}\right)^2 + \left(\frac{n\pi}{l_y}\right)^2\right]}, \tag{C20, C21}$$

$$\lambda^{(x)}_{m,n}(x, y) = \cos(m\pi x/l_x)\sin(n\pi y/l_y), \qquad \lambda^{(y)}_{m,n}(x, y) = \sin(m\pi x/l_x)\cos(n\pi y/l_y), \tag{C22, C23}$$

with $m = 0, 1, 2, \ldots$ and $n = 0, 1, 2, \ldots$. The out-of-plane force N_{z1} and the flexural moments M_{x1} and M_{y1} at position 1 generate flexural waves that at position 2 are

characterized by both transverse $\dot{w}_2$ velocity and angular $\dot{\theta}_{x2}$ and $\dot{\theta}_{y2}$ velocities. Therefore, the point mobility associated with this excitation are [20, 38, 49]

$$m^{21}_{wMx} = \frac{\dot{w}_2}{M_{x1}} = \mathrm{j}\omega \sum_{m=1}^{\infty}\sum_{n=1}^{\infty} \frac{\varphi_{m,n}(x_2, y_2)\psi^{(x)}_{m,n}(x_1, y_1)}{\Lambda[\omega^2_{fm,n}(1 + \mathrm{j}\eta) - \omega^2]}, \tag{C24}$$

$$m^{21}_{wMy} = \frac{\dot{w}_2}{M_{y1}} = \mathrm{j}\omega \sum_{m=1}^{\infty}\sum_{n=1}^{\infty} \frac{\varphi_{m,n}(x_2, y_2)\psi^{(y)}_{m,n}(x_1, y_1)}{\Lambda[\omega^2_{fm,n}(1 + \mathrm{j}\eta) - \omega^2}, \tag{C25}$$

$$m^{21}_{\theta xMx} = \frac{\dot{\theta}_{x2}}{M_{x1}} = \mathrm{j}\omega \sum_{m=1}^{\infty}\sum_{n=1}^{\infty} \frac{\psi^{(x)}_{m,n}(x_2, y_2)\psi^{(x)}_{m,n}(x_1, y_1)}{\Lambda[\omega^2_{fm,n}(1 + \mathrm{j}\eta) - \omega^2]}, \tag{C26}$$

$$m^{21}_{\theta xMy} = \frac{\dot{\theta}_{x2}}{M_{y1}} = \mathrm{j}\omega \sum_{m=1}^{\infty}\sum_{n=1}^{\infty} \frac{\psi^{(x)}_{m,n}(x_2, y_2)\psi^{(y)}_{m,n}(x_1, y_1)}{\Lambda[\omega^2_{fm,n}(1 + \mathrm{j}\eta) - \omega^2]}, \tag{C27}$$

$$m^{21}_{\theta yMy} = \frac{\dot{\theta}_{y2}}{M_{y1}} = \mathrm{j}\omega \sum_{m=1}^{\infty}\sum_{n=1}^{\infty} \frac{\psi^{(y)}_{m,n}(x_2, y_2)\psi^{(y)}_{m,n}(x_1, y_1)}{\Lambda[\omega^2_{fm,n}(1 + \mathrm{j}\eta) - \omega^2]}, \tag{C28}$$

$$m^{21}_{\theta yMx} = \frac{\dot{\theta}_{y2}}{M_{x1}} = \mathrm{j}\omega \sum_{m=1}^{\infty}\sum_{n=1}^{\infty} \frac{\psi^{(y)}_{m,n}(x_2, y_2)\psi^{(x)}_{m,n}(x_1, y_1)}{\Lambda[\omega^2_{fm,n}(1 + \mathrm{j}\eta) - \omega^2]}, \tag{C29}$$

$$m^{21}_{\theta xNz} = \frac{\dot{\theta}_{x2}}{N_{z1}} = \mathrm{j}\omega \sum_{m=1}^{\infty}\sum_{n=1}^{\infty} \frac{\psi^{(x)}_{m,n}(x_2, y_2)\varphi_{m,n}(x_1, y_1)}{\Lambda[\omega^2_{fm,n}(1 + \mathrm{j}\eta) - \omega^2]}, \tag{C30}$$

$$m^{21}_{\theta yNz} = \frac{\dot{\theta}_{y2}}{N_{z1}} = \mathrm{j}\omega \sum_{m=1}^{\infty}\sum_{n=1}^{\infty} \frac{\psi^{(y)}_{m,n}(x_2, y_2)\varphi_{m,n}(x_1, y_1)}{\Lambda[\omega^2_{fm,n}(1 + \mathrm{j}\eta) - \omega^2]}, \tag{C31}$$

$$m^{21}_{wNz} = \frac{\dot{w}_2}{N_{z1}} = \mathrm{j}\omega \sum_{m=1}^{\infty}\sum_{n=1}^{\infty} \frac{\varphi_{m,n}(x_2, y_2)\varphi_{m,n}(x_1, y_1)}{\Lambda[\omega^2_{fm,n}(1 + \mathrm{j}\eta) - \omega^2]}, \tag{C32}$$

where $\Lambda = \rho s l_x l_y/4$ is the modal mass, $\omega_{fm,n}$ is the m,nth natural frequency due to the flexural wave propagating on the plate, η is the loss factor, and $\varphi_{m,n}$, $\psi^{(x)}_{m,n}$ and $\psi^{(y)}_{m,n}$ are the m,nth eigenfunctions [38]:

$$\omega_{fm,n} = \sqrt{\frac{Es^2}{12\rho(1 - \nu^2)}}\left[\left(\frac{m\pi}{l_x}\right)^2 + \left(\frac{n\pi}{l_y}\right)^2\right], \qquad \varphi_{m,n}(x, y) = \sin\frac{m\pi x}{l_x}\sin\frac{n\pi y}{l_y}, \tag{C33, C39}$$

$$\psi^{(x)}_{m,n}(x, y) = \frac{n\pi}{l_y}\sin\frac{m\pi x}{l_x}\cos\frac{n\pi y}{l_y}, \qquad \psi^{(y)}_{m,n}(x, y) = -\frac{m\pi}{l_x}\cos\frac{m\pi x}{l_x}\sin\frac{n\pi y}{l_y}. \tag{C35, C36}$$

APPENDIX D: TRANSFORMATION MATRIX

In the model presented in section 2 two sets of vector parameters are considered: the *source–receiver velocity* or *force* vectors ($\mathbf{v}_{sr}$ $\mathbf{f}_{sr}$) defined by equations (16) and (17) and the *mounting system velocity* or *force* vectors ($\mathbf{v}_m$ $\mathbf{f}_m$) defined by equations (7) and (8). These

two sets of vectors are related to each other by the two following equations ensuring the equilibrium and continuity principles at the system junctions:

$$\mathbf{v}_m = \mathbf{T}\mathbf{v}_{sr}, \qquad \mathbf{f}_m = -\mathbf{T}\mathbf{f}_{sr}, \tag{D1}$$

The matrix **T**, called the transformation matrix, gives the relations between the source–receiver parameters and the mounting system parameters. Depending on the characteristics of the three members of the system, this matrix assumes a different form.

In this Appendix the transformation matrix **T** is presented for the system studied in this paper. As shown in Figure A1, when the mounts are not vertically oriented the mounting system vector parameters are rotated with reference to the source–receiver vector parameters, then the transformation matrix **T** has to relate all the "linear parameters"† of the mounting system vectors associated to a particular junction j with each "linear parameter" of the source receiver vectors of the same junction j. Another condition that the transformation matrix has to consider is the fact that the in-plane junction forces (N_{yj}) acting on the receiver plate act on the surface of the plate and then generate a moment acting on the receiver plate given by $N_{yj}s/2$. Therefore, the transformation matrix has to relate the projection on the y-axes of the mounting system vectors "linear parameters" associated with a particular receiver junction j_r to the angular parameter (rotation or moment) associated with the same junction j_r of the source receiver vector.

Upon considering these two types of conditions the transformation matrix is found to be given by

$$\mathbf{T} = \begin{bmatrix} \mathbf{T}_{ls} & \mathbf{0} & \mathbf{0} & \mathbf{0} \\ \mathbf{0} & \mathbf{T}_{rs} & \mathbf{0} & \mathbf{0} \\ \mathbf{0} & \mathbf{0} & \mathbf{T}_{lr} & \mathbf{0} \\ \mathbf{0} & \mathbf{0} & \mathbf{0} & \mathbf{T}_{rr} \end{bmatrix}, \tag{D2}$$

where

$$\mathbf{T}_{ls} = \begin{bmatrix} \cos\beta & \sin\beta & 0 \\ -\sin\beta & \cos\beta & 0 \\ 0 & 0 & 1 \end{bmatrix}, \qquad \mathbf{T}_{rs} = \begin{bmatrix} \cos\beta & -\sin\beta & 0 \\ \sin\beta & \cos\beta & 0 \\ 0 & 0 & 1 \end{bmatrix}, \tag{D3, D4}$$

$$\mathbf{T}_{lr} = \begin{bmatrix} \cos\beta & \sin\beta & 0 \\ -\sin\beta & \cos\beta & 0 \\ -(s/2)\cos\beta & -(s/2)\sin\beta & 1 \end{bmatrix}, \qquad \mathbf{T}_{rr} = \begin{bmatrix} \cos\beta & -\sin\beta & 0 \\ \sin\beta & \cos\beta & 0 \\ -(s/2)\cos\beta & (s/2)\sin\beta & 1 \end{bmatrix}, \tag{D5, D6}$$

where β is the mount inclination, s is the thickness of the plate and **0** is the 3×3 zero matrix.

‡ The linear parameters are considered to be the junction displacements w_j and v_j and the junction forces N_j and Q_j.